PDGFR ALPHA SIGNALING REQUIREMENTS IN THE DEVELOPMENT OF TISSUES DERIVED FROM SCLEROTOME AND DERMATOME

APPROVED BY SUPERVISORY COMMITTEE

Michelle Tallquist, Ph.D. (Mentor)

Hui Zou, Ph.D (Committee Chair)

Rueyling Lin, Ph.D.

Eric Olson, Ph.D.

DEDICATION

Thanks to Mom and Dad and all the family and friends who helped me get here,

especially my wonderful husband, Mark.

PDGFR ALPHA SIGNALING REQUIREMENTS IN THE DEVELOPMENT OF TISSUES DERIVED FROM SCLEROTOME AND DERMATOME

by

ELIZABETH ANN PICKETT

DISSERTATION

Presented to the Faculty of the Graduate School of Biomedical Sciences

The University of Texas Southwestern Medical Center at Dallas

In Partial Fulfillment of the Requirements

For the Degree of

DOCTOR OF PHILOSOPHY

The University of Texas Southwestern Medical Center at Dallas

Dallas, Texas

May, 2007

PDGFR ALPHA SIGNALING REQUIREMENTS IN THE DEVELOPMENT OF TISSUES DERIVED FROM SCLEROTOME AND DERMATOME

ELIZABETH ANN PICKETT, Ph.D.

The University of Texas Southwestern Medical Center at Dallas, 2007

MICHELLE TALLQUIST, Ph.D.

The Platelet-Derived Growth Factor Receptors (PDGFR) play roles in the development of multiple mesenchymal cell types. Upon ligand binding, the receptors signal through a number of intracellular signaling molecules and elicit many cellular responses including migration, proliferation, and differentiation. Studies utilizing tissue-specific deletion permit the elucidation of cell autonomous phenotypes, while analysis of signaling point mutants permits identification of the function of specific downstream effectors. My studies use both methods to uncover the role of PDGFRα signaling in the development of skin and bone.

An unexplained phenotype of PDGFRα null embryos is a defect in the axial skeletal that leads to spina bifida. Using conditional gene deletion I determined that the population of cells responsible for this phenotype is not the chondrocyte but is instead another derivative of the sclerotome. These results demonstrate that signals from adjacent tissues can play important roles in the differentiation of bone populations and identifies an etiology for spina bifida that is not directly caused by neural tube or bone defects.

Interestingly, loss of PI3K signaling downstream of PDGFRα also results in spina bifida. I found that the sclerotome population described above requires PDGFRα signaling to migrate dorsal to the neural tube via PI3K activation. Without this signaling event, downstream effectors including Akt, p70S6K, and PAK1 are not activated and the cells fail to form Rac-associated membrane ruffles. This is the first in vivo evidence that PI3K driven pathways are required for migration downstream of the PDGFRα.

The dermal deletion of PDGFRα leads to blister formation in multiple locations. Contrary, to what has been proposed, these membrane blisters are not due to dermal hypoplasia or dermal cell death. Instead, they are caused by a failure to maintain the dermal-epidermal junction (DEJ). In my analyses I show that Frem1, an important protein in establishing dermal/epidermal adhesion, is not maintained in the basal lamina. These data suggest that loss of PDGFRα signals from the dermis lead to a disruption of protein localization or complex formation at the DEJ.

The results obtained from these studies demonstrate that different cell populations utilize PDGFRα signaling in unique ways and careful analysis is required in each cell type to establish its dependence on this receptor tyrosine kinase.

TABLE OF CONTENTS

PRIOR PUBLICATIONS

Robert C. Anderson*, **Elizabeth A. Pickett***, Christopher L. Smith, Daiji Kiyozumi, Kiyotoshi Sekiguchi, and Michelle D. Tallquist. *PDGF receptor alpha deficient dermis exhibits Fraser syndrome-like epidermal blistering.* Submitted.

*These two authors contributed equally.

Elizabeth A. Pickett and Michelle D. Tallquist. *Disruption of PDGFRα initiated PI3 kinase migration leads to spina bifida.* Manuscript in preparation.

LIST OF FIGURES

LIST OF TABLES

LIST OF ABREVIATIONS

BrdU – 5-bromo-2-deoxyuridine

DEJ – Dermal-epidermal junction

EB – Epidermolysis bullosa

ECM – Extracellular matrix

EGF – Epidemal growth factor

IGF – Insulin-like growth factor

PAK1 – p21-activated kinase

PDGF – Platelet derived growth factor

PDGFR – Platelet derived growth factor receptor

PDK1 – 3-phosphoinositide-dependent kinase 1

PI3K – Phosphoinositide 3-kinase

CHAPTER ONE

Introduction

The PDGF receptors have long been known for their activities in mesenchymal cells, but little work has focused on the in vivo phenotypes related to the somite derivatives. This body of work focuses on the development of bone and skin defects that result from deficient PDGFRα signaling.

Somites give rise to multiple cell populations

Many of the tissues of the trunk region of vertebrate organisms are derived from somites during early embryogenesis (as reviewed in (1, 2)). Somites are epithelial bundles formed as buds of mesenchyme, from the unsegmented paraxial mesoderm, that undergo a mesenchymal to epithelial transformation. These cell bundles form in pairs on either side of the neural tube in a rostral to caudal fashion. The cells within each somite will differentiate into three distinct cell types: bone, muscle, and dermis. Initially, the epithelial bundle of cells will undergo epithelial to mesenchymal transformation and segregate into 2 portions, the scleretome and the dermomyotome.

The dermomyotome will form the dermis of the dorsum (from the dermatome) and the skeletal muscles of the vertebrate body (from the myotome) (reviewed by (3)). This epithelial sheet will initially sit in between the sclerotome and the surface ectoderm. The edges of these cell populations remain epithelial to enable ongoing myotomal growth even as the center, or dermatome, forms a loose

mesenchyme with cell migrating dorsally as dermal and subcutaneous precursor cells. As differentiation occurs, two somite-derived populations of dermis progenitor cells can be distinguished: one that expresses Msx1 and contributes to the dermis of the dorsalmost trunk region, and one that expresses Twist2, but not Msx1 and contributes to the dermis overlaying the dermomyotome (4).

The scleretome gives rise to the vertebral column and ribs, as well as the associated connective tissue. Each vertebral body is formed by the caudal half of one sclerotome and the cranial half of the caudally adjacent sclerotome in a process known as resegmentation (5-11), (and the articles in German from the 1800's reviewed by (12)). The neural arches are primarily formed from cells originating from the caudal half-somite, while the intervertebral discs arise from cells located in the cranial portion. The resegmented sclerotome partitions into subdomains that contain progenitors for specific future cell populations. These subdomains (and the cells they give rise to) are as follows: the syndetome (tendons of the epaxial domain) (13), the meningotome (blood vessels and meninges of the spinal cord) (14, 15), the arthrotome (intervertebral discs and joints of the vertebral column) (8) (so named in (16)), and the neurotome (perineurium and endoneurium which participate in the formation of dorsal root ganglia and spinal nerves) (17).

The remaining domains of the sclerotome are known as the ventral, central, and dorsal sclerotome (as reviewed in (14, 16)). The central or lateral

part develops into the pedicles and ventral parts of the neural arches as well as the proximal ribs. The ventral portion begins as an extracellular matrix-containing domain free of cells. This space is invaded by sclerotomal cells that proliferate and become the vertebral bodies and the intervertebral discs. Finally, the late developing dorsal sclerotome migrates and invades the space between the surface ectoderm and the neural tube, where it will form the dorsal portion of the neural arches and the spinous process.

Endochondral bone formation from sclerotome

The bones of the vertebral column arise from the scleretome portion of the somite and form by endochondral ossification. In this process, sclerotome cells differentiate into chondrocytes, which in turn go through three stages of differentiation: proliferative, pre-hypertrophic, and hypertrophic. Large hypertrophic chondrocytes secrete cartilage matrix and then undergo apoptosis. These cells are replaced by invading osteoblasts, the cells that produce calcified bone.

While endochondral ossification has been studied in great detail in the long bone (as reviewed in (18, 19)), little has been reported on irregular bones like the vertebral arches. In long bone, round proliferative chondrocytes produce type II collagen and form a columnar layer. They then flatten, cease proliferating and become rounded prehypertrophic chondrocytes, upregulating Ihh and Runx2 in

the process (20, 21). These cells continue to enlarge and differentiate into post-mitotic hypertrophic cells that express type X collagen and mineralize the surrounding matrix (22, 23). This is followed by the death of the hypertrophic chondrocytes, blood vessel invasion, and the replacement of the cartilaginous matrix by trabecular bone (primary spongiosa) (24). The primary center splits into two opposite growth plates, in each of which the maturation of cartilage and remodeling into bone continues as long as new chondrocytes are generated in the growth plates.

Analysis of the signaling involved in arch development has been primarily conducted in the chick utilizing the chick-quail chimera system. Studies conducted investigated the roles of the neural tube and notochord in the development of the vertebral column. Findings suggest BMP4 secretion from the roof plate of the neural tube is essential for promoting arch development while Shh secreted by the notochord is necessary for rib development (25).

Dermis and Epidermis Formation

The dorsal dermis arises from cells of the dermatome portion of the somite, while the overlying epidermis develops from the surface ectoderm. The cutaneous basement membrane is located between the epidermis and the dermis of the skin and is known as the dermal-epidermal junction (DEJ) (reviewed by

(26)). The DEJ separates these two layers and provides adhesion between them, thereby maintaining the structural integrity of the skin. The exact functions of the protein components of the DEJ are not yet fully understood, but defects in several of these molecules have been associated with a group of heritable skin diseases, characterized by blistering of the skin, termed epidermolysis bullosa (EB) (27).

Fraser syndrome is an EB-like disorder characterized by blistering of the fetal epidermis, cryptophthalmos, syndactyly, and renal agenesis (28-30). Genetic mapping of loci from mouse models for Fraser syndrome has revealed several new proteins required for dermal-epidermal adhesion during embryonic development (31, 32). The FRAS/FREM gene family (Fras1, Frem1/QBRICK, and Frem2) are extracellular matrix components that partipate in dermal-epidermal junctions, while Grip1 is an adaptor protein that interacts with Fras1 (27-29, 33-35). While genetic studies have demonstrated roles for these proteins in the epidermis for maintenance of adhesion, less is known about the contribution of the proteins from the dermis in DEJ interactions.

PDGF-A is expressed in the developing epidermis and hair follicle epithelium while PDGFRα is expressed in the associated mesenchyme structures, like the dermis. PDGFRα null embryos develop multiple epidermal blebs and dermal hypoplasia, suggesting a role for the PDGFRα in the development of the dermis (36). Karlsson, et al (37) characterized the skin and hair of mice null for PDGF-A. The mutant mice have thinner dermis, misshapen hair follicles, smaller

dermal papillae, abnormal dermal sheaths and thinner hair when compared to littermate controls. Reduced BrdU labeling in the dermis and dermal sheaths of null mice led to the proposal that PDGF-A has a role in stimulating proliferation of the PDGFRα-expressing dermal mesenchymal cells.

Platelet Derived Growth Factor (PDGF)

Deletion studies in mice have demonstrated the requirement for PDGF signaling during embryonic development as null mutations of either PDGFR result in embryonic lethality. PDGFRα signals are required for the proper development of a number of mesenchymal cell types including chondrocytes, oligodendrocytes, lung alveolar smooth muscle, and kidney (36, 38-41). The PDGFRα null mutation is embryonic lethal and mutant embryos display phenotypes as early as e10.5 including hemorrhagic blebbing in multiple locations, edema, craniofacial clefting, and axial skeleton malformations (36). In contrast, PDGFRβ signaling appears most important for the development of smooth cell populations (42-44). PDGFRβ null mice appear healthy until e16-19, at which time they die from cardiovascular complications due to dilation of the heart and large blood vessels and rupture of the capillaries (42).

In many tissues during organogenesis, PDGFRα is expressed in the mesenchyme while its ligands, PDGFC and PDGFA, are expressed by the overlying epithelium (37, 45-47). PDGFA expression within the developing

somite is dynamic. At E8-9.5, it is expressed in the central domain of the early somite (38). As the somite differentiates, PDGRA expression becomes more restricted to the myotome, where it signals to the PDGFRα expressed in the sclerotome. PDGFRβ is expressed in vascular smooth muscle and pericyte progenitor cells, while PDGF-B has highest expression in associate endothelium (48).

Platelet-derived growth factor (PDGF) signaling is achieved by the interactions of the ligands and receptors of the PDGF family (see (49, 50) for reviews). Four genes (A, B, C, and D) encode the proteins that dimerize to form five active forms of the ligand (AA, AB, BB, CC, and DD). The receptors are encoded by two genes (α and β) whose resulting proteins dimerize to form the three active receptor complexes (αα, αβ, and ββ). Binding of a ligand to its receptor stimulates autophosphorylation of the receptor tyrosine kinase and activation of downstream signaling targets including Src, PI3K, PLCγ, and Ras. These downstream signaling cascades can in turn promote cell proliferation, survival, and migration.

Downstream Signaling Leads to Cell Migration

One of the key signaling targets downstream of PDGFR is the phosphoinositide 3-kinase (PI3K) pathway. PI3K is brought to the membrane and activated via binding to phosphotyrosine residues of growth factor receptors such

as PDGFR. The product of PI3K, phosphatidylinositol-3,4,5-triphosphate (PIP_3), recruits proteins such as Akt, PDK1, Grp1, and Rac to the membrane where they are activated. These proteins are then capable of initiating signal transduction cascades that direct protein synthesis, actin polymerization, cell survival, and cell cycle entry (51). Signaling point mutant mouse strains have been designed that allow analysis of individual pathways downstream of the PDGF receptors. These mutants, termed the "F-series," have tyrosine-to-phenylalanine point mutations that prohibit binding by removing the phosphotyrosine residues (52).

The involvement of PI3K in chemotaxis has been analyzed in vitro downstream of a number of cytokines including PDGF, IGF, EFG, and integrins (53-56). Utilizing wortmannin or LY294002 to inhibit PI3K activity, multiple cell types have been shown to lose coordinated migration capabilities. The most common pathway in which PI3K is thought to participate in migration is through activation of Rac downstream of Akt (56, 57).

Rac1, a small GTPase, is a member of the Rho family of proteins. Rac1 can be activated by factors such as PDGF or insulin, leading to the formation of a network of actin filaments at the cell periphery to form lamellipodia and membrane ruffles (58). Surprisingly, the Rac1 null is still capable of migrating in response to PDGF stimulation, despite a lack of membrane ruffles and an inability to form lamellipodia (59). Binding of active Rac1 is thought to be necessary for full activation of p21-activated kinase 1 (PAK1), a molecule involved in many

cellular functions including polarized morphogenesis of the actin cytoskeleton (60). Current models of PAK1 activation suggest multiple events regulate activity. PAK1 must be phosphorylated by PDK1 and must bind the PKB domain of activated Rac1 to undergo a conformational change and autophosphorylation (61, 62).

Summary

In chapter 2, I investigate the role of PDGFRα in the development of the vertebral arch. Mice deficient in PI3K signaling downstream of PDGFRα displayed a spina bifida phenotype due to failure of the arches to fully form. Conditional mutant analysis revealed that this phenotype was not due to a defect within the developing bone, but instead was caused by failure of the adjacent mesenchyme to migrate dorsal to the neural tube. In vitro analysis demonstrated that PI3K signaling is necessary for a migratory response to PDGF-A and for phosphorylation of PAK1, a molecule associated with cytoskeletal actin organization. These results reveal a cell population that relies on PDGFRα signaling in vivo solely for migration and demonstrates that PDGFRα association with PI3K leads to PAK1 phosphorylation, suggesting that failure of this activation may result in failed migration.

In chapter 3, we determine the requirement of PDGFRα signaling in the dermis for maintenance of dermal-epidermal adhesion. Embryos lacking

PDGFRα in the dermis formed subepidermal blisters similar to those observed in the human disorder Fraser syndrome. Section analysis indicated that this defect was not due to failure to form dermis, but by a failure to maintain specific extracellular matrix molecules at the basement membrane. While many matrix molecules were deposited normally in this region, a progressive loss of FREM1 localization was observed as dermal development progressed. This suggests that PDGFRα-mediated events are required during dermis development to form dermal-epidermal adhesion.

In chapter 4, I describe the effects of deficient PDGF signaling on bone development. PDGFR mutants lacking PI3K signaling downstream of both receptors had increased apoptosis within the somites at e10.5 and a disorganized chondrocyte phenotype within the vertebral body, rib, and scapula at e12.5. Deletion of the receptors within the chondrocytes resulted in a misaligned sternum and a potential alteration in the differentiation of the chondrocytes within the vertebral body.

Together these studies reveal specific in vivo roles for PDGFR signaling during embryonic development. Lack of PDGFRα signaling in the dermis causes a disruption of the dermal-epidermal junction even though the dermis forms properly. Interestingly, aberrant PDGF signaling can have both a direct and an indirect effect on some tissues, like the bone. In the case of the sternum misalignment (due to loss of PDGFR signaling in the chondrocytes) and the spina

bifida (due to loss of PI3K signaling downstream of PDGFRα in the mesenchyme) phenotypes, the cause might ultimately be the same: failure of a cell population to migrate properly. The results obtained from these experiments lead to a better understanding of the roles of the PDGF receptors in the direction of cellular functions and help determine the function of PI3K downstream of the receptors in different cell types.

References

1. Yusuf, F. & Brand-Saberi, B. (2006) Anat Embryol (Berl) 211 Suppl 1, 21-30.

2. Christ, B. & Ordahl, C. P. (1995) Anat Embryol (Berl) 191, 381-396.

3. Scaal, M. & Christ, B. (2004) Anat Embryol (Berl) 208, 411-424.

4. Houzelstein, D., Cheraud, Y., Auda-Boucher, G., Fontaine-Perus, J., & Robert, B. (2000) Development 127, 2155-2164.

5. Bagnall, K. M., Higgins, S. J., & Sanders, E. J. (1988) Development 103, 69-85.

6. Bagnall, K. M., Higgins, S. J., & Sanders, E. J. (1989) Development 107, 931-943.

7. Huang, R., Zhi, Q., Wilting, J., & Christ, B. (1994) Anat Embryol (Berl) 190, 243-250.

8. Huang, R., Zhi, Q., Neubuser, A., Muller, T. S., Brand-Saberi, B., Christ, B., & Wilting, J. (1996) Acta Anat (Basel) 155, 231-241.

9. Huang, R., Zhi, Q., Schmidt, C., Wilting, J., Brand-Saberi, B., & Christ, B. (2000) Development 127, 527-532.

10. Ewan, K. B. & Everett, A. W. (1992) Exp Cell Res 198, 315-320.

11. Aoyama, H. & Asamoto, K. (2000) Mech Dev 99, 71-82.

12. Brand-Saberi, B. & Christ, B. (2000) Curr Top Dev Biol 48, 1-42.

13. Brent, A. E., Schweitzer, R., & Tabin, C. J. (2003) Cell 113, 235-248.

14. Christ, B., Huang, R., & Wilting, J. (2000) Anat Embryol (Berl) 202, 179-194.

15. Halata, Z., Grim, M., & Christ, B. (1990) Anat Embryol (Berl) 182, 529-537.

16. Christ, B., Huang, R., & Scaal, M. (2004) Anat Embryol (Berl) 208, 333-350.

17. Christ, B., Jacob, H. J., & Jacob, M. (1975) Verh Anat Ges 69, 259-261.

18. Karsenty, G. & Wagner, E. F. (2002) Dev Cell 2, 389-406.

19. Provot, S. & Schipani, E. (2005) Biochem Biophys Res Commun 328, 658-665.

20. Sakaguchi, T., Kuroiwa, A., & Takeda, H. (2001) Mech Dev 107, 25-38.

21. Ueta, C., Iwamoto, M., Kanatani, N., Yoshida, C., Liu, Y., Enomoto-Iwamoto, M., Ohmori, T., Enomoto, H., Nakata, K., Takada, K., et al. (2001) J Cell Biol 153, 87-100.

22. Linsenmayer, T. F., Chen, Q. A., Gibney, E., Gordon, M. K., Marchant, J. K., Mayne, R., & Schmid, T. M. (1991) Development 111, 191-196.

23. Poole, C. A., Glant, T. T., & Schofield, J. R. (1991) J Histochem Cytochem 39, 1175-1187.

24. Gerber, H. P., Vu, T. H., Ryan, A. M., Kowalski, J., Werb, Z., & Ferrara, N. (1999) Nat Med 5, 623-628.

25. Monsoro-Burq, A. H. & Le Douarin, N. (2000) Curr Top Dev Biol 48, 43-75.

26. Burgeson, R. E. & Christiano, A. M. (1997) Curr Opin Cell Biol 9, 651-658.

27. Bladt, F., Tafuri, A., Gelkop, S., Langille, L., & Pawson, T. (2002) Proc Natl Acad Sci U S A 99, 6816-6821.

28. McGregor, L., Makela, V., Darling, S. M., Vrontou, S., Chalepakis, G., Roberts, C., Smart, N., Rutland, P., Prescott, N., Hopkins, J., et al. (2003) Nat Genet 34, 203-208.

29. Gattuso, J., Patton, M. A., & Baraitser, M. (1987) J Med Genet 24, 549-555.

30. Vrontou, S., Petrou, P., Meyer, B. I., Galanopoulos, V. K., Imai, K., Yanagi, M., Chowdhury, K., Scambler, P. J., & Chalepakis, G. (2003) Nat Genet 34, 209-214.

31. Winter, R. M. (1990) Clin Genet 37, 494-495.

32. Center, E. M. & Emery, K. E. (1997) Histol Histopathol 12, 901-907.

33. Smyth, I., Du, X., Taylor, M. S., Justice, M. J., Beutler, B., & Jackson, I. J. (2004) Proc Natl Acad Sci U S A 101, 13560-13565.

34. Takamiya, K., Kostourou, V., Adams, S., Jadeja, S., Chalepakis, G., Scambler, P. J., Huganir, R. L., & Adams, R. H. (2004) Nat Genet 36, 172-177.

35. Jadeja, S., Smyth, I., Pitera, J. E., Taylor, M. S., van Haelst, M., Bentley, E., McGregor, L., Hopkins, J., Chalepakis, G., Philip, N., et al. (2005) Nat Genet 37, 520-525.

36. Soriano, P. (1997) Development 124, 2691-2700.

37. Karlsson, L., Bondjers, C., & Betsholtz, C. (1999) Development 126, 2611-2621.

38. Tallquist, M. D., Weismann, K. E., Hellstrom, M., & Soriano, P. (2000) Development 127, 5059-5070.

39. Fruttiger, M., Karlsson, L., Hall, A. C., Abramsson, A., Calver, A. R., Bostrom, H., Willetts, K., Bertold, C. H., Heath, J. K., Betsholtz, C., et al. (1999) Development 126, 457-467.

40. Bostrom, H., Willetts, K., Pekny, M., Leveen, P., Lindahl, P., Hedstrand, H., Pekna, M., Hellstrom, M., Gebre-Medhin, S., Schalling, M., et al. (1996) Cell 85, 863-873.

41. Li, X., Ponten, A., Aase, K., Karlsson, L., Abramsson, A., Uutela, M., Backstrom, G., Hellstrom, M., Bostrom, H., Li, H., et al. (2000) Nat Cell Biol 2, 302-309.

42. Soriano, P. (1994) Genes Dev 8, 1888-1896.

43. Lindahl, P., Johansson, B. R., Leveen, P., & Betsholtz, C. (1997) Science 277, 242-245.

44. Lindahl, P., Hellstrom, M., Kalen, M., Karlsson, L., Pekny, M., Pekna, M., Soriano, P., & Betsholtz, C. (1998) Development 125, 3313-3322.

45. Takakura, N., Yoshida, H., Kunisada, T., Nishikawa, S., & Nishikawa, S. I. (1996) J Invest Dermatol 107, 770-777.

46. Ding, H., Wu, X., Kim, I., Tam, P. P., Koh, G. Y., & Nagy, A. (2000) Mech Dev 96, 209-213.

47. Ansel, J. C., Tiesman, J. P., Olerud, J. E., Krueger, J. G., Krane, J. F., Tara, D. C., Shipley, G. D., Gilbertson, D., Usui, M. L., & Hart, C. E. (1993) J Clin Invest 92, 671-678.

48. Hellstrom, M., Kalen, M., Lindahl, P., Abramsson, A., & Betsholtz, C. (1999) Development 126, 3047-3055.

49. Tallquist, M. & Kazlauskas, A. (2004) Cytokine Growth Factor Rev 15, 205-213.

50. Betsholtz, C. (2004) Cytokine Growth Factor Rev 15, 215-228.

51. Cantley, L. C. (2002) Science 296, 1655-1657.

52. Klinghoffer, R. A., Hamilton, T. G., Hoch, R., & Soriano, P. (2002) Dev Cell 2, 103-113.

53. Rosenmuller, T., Rydh, K., & Nanberg, E. (2001) J Cell Physiol 188, 369-382.

54. Fujita, T., Azuma, Y., Fukuyama, R., Hattori, Y., Yoshida, C., Koida, M., Ogita, K., & Komori, T. (2004) J Cell Biol 166, 85-95.

55. Qiu, Q., Yang, M., Tsang, B. K., & Gruslin, A. (2004) Mol Hum Reprod 10, 677-684.

56. Qian, Y., Zhong, X., Flynn, D. C., Zheng, J. Z., Qiao, M., Wu, C., Dedhar, S., Shi, X., & Jiang, B. H. (2005) Oncogene 24, 3154-3165.

57. Welch, H. C., Coadwell, W. J., Stephens, L. R., & Hawkins, P. T. (2003) FEBS Lett 546, 93-97.

58. Hall, A. (1998) Science 279, 509-514.

59. Vidali, G., Roser, J. E., Ling, L., Congiu, E., Manico, G., & Pirronello, V. (2006) Faraday Discuss 133, 125-135; discussion 191-230, 449-152.

60. Sells, M. A., Knaus, U. G., Bagrodia, S., Ambrose, D. M., Bokoch, G. M., & Chernoff, J. (1997) Curr Biol 7, 202-210.

61. Knaus, U. G. & Bokoch, G. M. (1998) Int J Biochem Cell Biol 30, 857-862.

62. Knaus, U. G., Wang, Y., Reilly, A. M., Warnock, D., & Jackson, J. H. (1998) J Biol Chem 273, 21512-21518.

CHAPTER TWO

Disruption of PDGFR alpha Initiated PI3 Kinase Migration Leads to Spina bifida

Abstract

Spina bifida is a common congenital malformation in humans that is often synonymous with neural tube defects (NTD). The mechanisms underlying this birth anomaly have not been completely elucidated, and it is likely that multiple etiologies exist. Exposure of chick embryos to the PDGF receptor inhibitor, imatinib, results in spina bifida without NTD. In a mouse model, loss of PDGFRα signal transduction through the phosphatidyl-inositol 3' kinase (PI3K) pathway leads to a defect in migration of a mesoderm population that directs vertebra development. Loss of PI3K activation leads to a reduction in rac1 localization to membrane ruffles and a failure in activation of Pak1, an actin nucleation factor. Taken together these results indicate that the PDGFRα activation of PI3K is essential for cell migration and failure in migration of this cell population leads to spina bifida.

Introduction

Migration is an essential process during embryonic development and also has roles in adult tissues. While PDGF receptors can induce cytoskeletal rearrangements and migration in vitro, only a few examples have been described in vivo. In Xenopus embryos, PDGFRα directs mesoderm toward the blastocoel roof (1). Disruption of this signaling pathway leads to randomized movement of cells. In drosophila PVR, a receptor tyrosine kinase related to the mammalian PDGF and VEGF receptors directs border cell migration to the oocyte (2).

PDGF receptor stimulation activates multiple downstream pathways that direct actin reorganization and cell motility. PI3K and PLCγ have been implicated in actin ruffle formation and cell motility driven by PDGFRβ stimulation in vitro (3-6), but loss of PI3K activation downstream of this receptor in vivo resulted in no obvious migration phenotype (6). Recently, PDGF receptor activation of Src has been shown to stimulate actin reorganization and lamellipodial extension. This activity is dependent on cortactin, Abl, and Arg activation (7). Currently, there is controversy over the ability of PDGFRα to direct cell migration. In fibroblasts or hematopoeitic cells stimulation of the PDGFRα leads to migration, but in transfected porcine aortic endothelial cells it does not (8-11).

Failure of neural tube closure is commonly believed to be the major cause of spina bifida. Spina bifida is a congenital birth defect where the vertebrae fail to

protect the spinal cord, and there are three common forms that vary in severity (occulta, meningocele, and myelomeningocele) (12). Two etiologies for spina bifida have been proposed. One category is failure in neural tube closure, also known as NTD (reviewed by (13)). The second category is failure of the sclerotome-derived mesenchyme surrounding the neural tube to proliferate or differentiate (14). Little is known about how the cell population adjacent to the vertebral arch can influence bone development. Previous analyses of the PDGFRα null and mutant alleles have demonstrated that loss of PDGFRα signaling results in spina bifida (14-16). We have used conditional and signaling point mutant alleles to determine the cause of spina bifida downstream of the PDGFRα.

In this report we demonstrate that defective migration leads to failed vertebral closure. Normal vertebral arch formation requires PDGFα signal transduction, and surprisingly the cell population dependent on this receptor is not the chondrocyte. We further show that disruption of PDGFRα signaling through PI3K also results in spina bifida. It is likely that the disruption of PI3K leads to a failure in Rac and Pak1 activation. These findings demonstrate that certain cell populations require PDGFα-induced PI3K activity for migration in vivo.

Results

Treatment with imatinib mesylate recapitulates PDGFRα spina bifida phenotype

One of the most widely accepted causes of spina bifida is failure of neural tube closure (13) but several PDGF receptor mutant alleles exhibit spina bifida without any evidence of neural tube defects. To determine if disruption of PDGF receptor activity can cause spina bifida after neural tube closure has occurred, we employed a pharmacological inhibitor of PDGF receptor tyrosine kinase activity (imatinib mesylate) to developing embryos (17). Using the avian system we treated Hamburger stage 14-17 embryos (just after neural tube closure, equivalent to an e11.5-12.5 mouse embryo) with imatinib mesylate. We then examined the vertebral formation in the embryos at stage 36 by histology. Imatinib mesylate-treated embryos exhibited failure of the lamina (plates of bone that form the posterior wall of the vertebrae) to extend to the dorsal midline in the lumbar and lumbar sacral regions in all treated embryos, while all vehicle-treated embryos possessed normal vertebral development (Fig. 1). Other tissues of the drug-treated embryos, including the cranial-facial region and limbs, appeared normal with the exception of two embryos. In two embryos treated with the higher dose of drug, we also observed failure of ventral closure, which has also been reported in PDGFRα null embryos (16). These data suggested that inhibition of PDGF receptor signaling after neural tube closure could lead to spina bifida.

Loss of PDGFRα from cartilage does not result in spina bifida

The lumbar vertebrae form by extension of the somite-derived sclerotome around the neural tube. PDGFRα is expressed in the epithelial somite but becomes restricted to a subset of cells including the perichondrium, the condensing mesenchyme surrounding the vertebral disc, and the dermis (14, 18-20). To gain a better understanding of the cellular disruption leading to spina bifida in PDGFRα mutant embryos, we examined mice with either a tissue specific deletion of the receptor or a signaling point mutation. To delete PDGFRα from cartilage populations, we crossed mice bearing the *PDGFRα* conditional allele (21) to mice that express Cre recombinase driven by the *Col2a1* promoter (22) (referred to as PDGFRα^{CKO}). In these embryos, Cre is expressed in the sclerotome as early as E9.5 and results in recombination of *loxP*-flanked alleles in all cartilage and perichondrium of the axial skeleton (23). We also generated mice with a broader deletion in the somite derivatives by crossing our PDGFRα conditional animals to mice with expression of Cre from the *Twist2* locus (24) (referred to as PDGFRα^{TKO}). In this mouse line Cre is expressed in the sclerotome condensing mesenchyme, the dermatome, and osteoblasts. We also examined embryos expressing a PDGFRα that was incapable of signaling through PI3K (PDGFRα$^{PI3K/PI3K}$) and had been previously reported to display a spina bifida phenotype (15). This allele contains engineered point mutations in the domain of

the PDGFRα that normally binds PI3K, resulting in a loss of this signaling pathway downstream of the receptor.

Skeletal preparations demonstrated that loss of PDGFRα in chondrocytes resulted in completely normal formation of the vertebrae (Fig. 2B) when compared to controls (Fig. 2A). In contrast, although the vertebral bodies, vertebral arches and pedicles formed normally in PDGFRα^{TKO} and PDGFRα$^{PI3K/PI3K}$ embryos, defects were observed in the dorsal-most sclerotome derivatives. In the lumbar region the progression of the lamina was significantly impeded, and the spinous process was absent in the lumbar region of these embryos (Fig. 2C-D). This phenotype was specific to the lumbar vertebrae (L1-L6) and sometimes included the immediate adjacent thoracic (T10-13) and sacral (S1-2) vertebrae. In all embryos examined the ribs and appendicular skeleton developed normally (Fig. 2). Interestingly, the vertebral arch defects in the *Twist2* conditional embryos were more severe than that observed in the *PDGFRα$^{PI3K/PI3K}$* embryos. Because of the non-overlapping phenotypes of the *PDGFRα^{CKO}* and the *PDGFRα^{TKO}* embryos, we concluded that the defect in lamina development was not a primary defect in perichondrium nor chondrocytes. Instead, the defect was likely caused by a loss of PDGFRα signaling in an adjacent sclerotome-derived cell population.

Loss of progression of the dorsal vertebrae

Because spina bifida is commonly associated with NTD, we examined the PDGFRα^{TKO} and PDGFRα$^{PI3K/PI3K}$ embryos throughout gestation for neural tube closure and found that the neural tube had a normal morphology and closed at the expected time point (Fig. 3). To identify when the defect in vertebral development appeared, we examined the lumbar region for cartilage by Safranin O staining between E14.5 and E18.5 (Fig. 3). At E14.5, control, PDGFRα$^{PI3K/PI3K}$, and PDGFRα^{TKO} embryos appeared similar, but by E15.5 and thereafter, the lamina of mutant embryos failed to progress (Fig. 3A-B, E-F, I-L). In wild type embryos the chondrocytes elongated along the dorsal aspect of the neural tube, but in mutant embryos small condensations of unstained mesenchyme were observed. By E16.5 the mesenchymal condensations could be identified, but the area was dramatically reduced and contained few chondrocytes. It appeared that the chondrocyte precursors of the lamina were present, but they failed to progress towards the dorsal midline.

Mesenchymal cell-secreted factors promote chondrogenesis

Previous reports suggested that growth factor secretion from adjacent tissues could affect the development of the dorsal vertebrae (25). To investigate the possibility that loss of PDGFRα signaling affected expression of chondrocyte growth factors, we isolated the primary cells from the lumbar region of E13.5 control, PDGFRα$^{PI3K/PI3K}$, and

PDGFRα^{TKO} embryos (see Material and Methods) and compared their abilities to promote chondrogenic growth and differentiation. We stimulated limb bud chondrocyte micromass cultures with conditioned media from these cells. Conditioned media from wild type and PDGFRα mutant cells were both capable of inducing cartilage proteoglycans similar to stimulation with TGFβ1 as measured by Alcian blue binding (Fig. 4). To determine if chondrocyte induction was specific to these primary cells we also tested conditioned media from mouse embryonic fibroblasts and HEK293 epithelial cell lines. Fibroblasts conditioned media did promote chondrocyte differentiation, while HEK293 induction was similar to media control. These data indicated that these primary cells were capable of secreting chondrogenic factors and that PDGFRα expression or signaling was not required for this secretion.

Disrupted sclerotome migration in PDGFRα mutant embryos

A major function of the PDGFRα during development is to promote the proliferation of progenitor cell populations. To determine if a proliferation defect was the cause of the aberrant vertebral formation, we compared proliferation of control and PDGFRα$^{PI3K/PI3K}$ embryos at E14.5. Both exhibited similar rates of proliferation in the chondrocytes of the neural arch as well as the loose sclerotome cells adjacent to the developing vertebrae and the dermis (Figure 8). We also investigated the proliferation of primary cells from E13.5 embryos and found that while control and PDGFRα cells proliferated in response to media containing 10% serum, in response to PDGFAA stimulation neither control nor

PDGFRα$^{PI3K/PI3K}$ cells proliferated above background. We also examined the mutant embryos for apoptotic cells and found that mutant and control embryos possessed similar numbers of TUNEL positive cells. These data suggested that cell survival and proliferation were normal in the PDGFRα$^{PI3K/PI3K}$ embryos.

When we examined the vertebral arch formation by Safranin O and H&E staining, we observed that a mesenchymal cell population migrated to the region dorsal to the neural tube between E14.5 and E15.5 in control embryos. In contrast this cell population was absent in the PDGFRα$^{PI3K/PI3K}$ embryos (Fig. 3 C-D, G-H). When we examined the lumbar region of E18.5 PDGFRα^{TKO} embryos we found a similar result. While the dermis layer was similar to control section with regards to thickness and hair follicle formation, a dramatic reduction of cells existed between the neural tube and the dermal layer (Fig. 3 K-L). In controls, we observed not only the developing vertebrae but also a dense mesenchyme directly adjacent to these cells. In PDGFRα^{TKO} embryos both cell populations were absent.

To determine which cell populations expressed the PDGFRα, we examined embryos that expressed GFP from the PDGFRα locus (PDGFRα^{GFP}). The GFP expression can be used to reliably trace the receptor expression (20). Sections of E14.5 control embryos demonstrated the location of PDGFRα expressing cells in the lumbar region. The most abundant receptor expression was in the mesenchyme surrounding developing vertebrae and in the dermis.

Receptor expression was also present in the perichondrium, but only a low expression level was observed in the developing chondrocytes (Fig. 5). A similar expression pattern has been reported previously for PDGFRα transcripts (14). In PDGFRα$^{GFP/+}$ embryos, the mesenchyme immediately adjacent to the forming arch had advanced to the extent of the tip of the vertebral arch. In contrast, in embryos possessing one PI3K allele and one GFP allele the population of GFP positive cells was present lateral to the vertebral arch but the majority of cells had not advanced even half the distance of the vertebral arch. These results suggested that PDGFRα signaling could be required for migration of this cell population.

To examine the ability of PDGF receptor stimulation to induce migration in this cell population, we tested primary cells from embryos whose genotypes were either *PDGFRα$^{PI3K/GFP}$* or *PDGFRα$^{GFP/+}$*. While cells isolated from wild type embryos migrated towards PDGF ligands and serum, mutant cells had a reduced ability to migrate towards PDGFAA and PDGFBB (Fig. 6). The mutant cells were still capable of migration as evidenced by their ability to migrate toward serum. These results indicated that loss of PI3K signals downstream of the PDGFRα leads to a migration defect.

Normal FAK phosphorylation but aberrant Akt and P70S6K phosphorylation

The role of PDGFRα in cell motility and actin reoganization actin varies depending on the cell population being examined (26), and PDGF-induced cell motility is controlled by multiple pathways. We determined if any of these pathways were affected in the PDGFRαPI3K cells. Focal adhesion kinase (FAK) phosphorylation and ERK phosphorylation have been associated with establishment of focal adhesions and actin reorganization, respectively. Therefore, we determined if either of these was affected by the $PDGFR\alpha^{PI3K/PI3K}$. Phosphorylation of these two components was comparable in mutant and control samples. This data was in agreement with previous analysis of MEF cells isolated from the $PDGFR\alpha^{PI3K/PI3K}$ embryos that suggested the PI3K mutation did not disrupt other signaling pathways downstream of the PDGFRα (15). Activation of PI3K by PDGFRα leads to multiple downstream events that regulate cell migration. To investigate which of these were disrupted in the $PDGFR\alpha^{PI3K/PI3K}$ cells we performed western blot analysis to determine the activation state of two of these downstream molecules. We found that the phosphorylation of AKT (Ser 473) and p70 S6kinase (Thr 389) was drastically reduced in the $PDGFR\alpha^{PI3K/PI3K}$ cells in response to PDGFAA stimulation (Fig. 7). To determine if the lack or p70 S6 kinase was related to the migration defect that we observed we tested the migratory capacity of the primary cells in the presence of rapamycin. Rapamycin

inhibits the mTORC1 complex that is upstream of p70 S6 kinase. Treatment of primary cells with rapamycin inhibited the ability of these cells to migrate towards PDGF ligands. Reduced migration was also observed when the chemoattractant was either bFGF or TGFβ1 (Figure 9). In contrast, rapamycin had no effect on the migration of these cells towards serum. These results are similar to those observed in vascular smooth muscle cells (27) and suggest that the rapamycin sensitive pathway is also involved in cytokeletal rearrangements.

Because both Akt and p70 S6 kinase have been associated with Rac activation, we next investigated a downstream effector of activated Rac, p21-activated kinase (Pak). Pak proteins are serine/threonine kinase effectors of Rho family GTPases (28, 29). Upon Rac binding Pak1 becomes autophosphorylated on serine 199 and threonine 204. Using a phosphospecific antibody, we found that PAK1 autophosphorylation was decreased. Because Pak1 can also be directly phosphorylated on threonine 423 by phosphoinositide dependent kinase 1 (PDK1) downstream of PI3K activity, we investigated this event via western blot and observed a lack of phosphorylation on 423 in response to PDGF stimulation in $PDGFR\alpha^{PI3K/PI3K}$ primary cells. In contrast, when these same cells are stimulated with serum containing media we observe phosphorylation of Pak1 by both phospho-specific antibodies demonstrating that these pathways are intact downstream of other signaling pathways. These data demonstrate that PDGFRα

association with PI3K leads to Pak1 phosphorylation and suggests that failure of this activation may result in faulty migration.

Discussion

Failure of neural tube closure is commonly believed to be the major cause of spina bifida. In this report we demonstrate that defective migration of a somite population leads to failed vertebrae closure. Normal vertebral arch formation requires PDGFRα signal transduction, and surprisingly the cell population dependent on PDGFRα is not the chondrocyte. We further show that disruption of PDGFRα signaling through PI3K also results in spina bifida. We provide evidence that cells derived from the $PDGFR\alpha^{PI3K/PI3K}$ embryos have a migration defect. Downstream signaling through both Akt and p70 S6 kinase was disrupted in these cells, and a key actin nucleation factor Pak1 is rendered inactive. Although p70 S6 kinase and PI3K activity have been linked to Rac activation, it is unlikely that Rac is the only disrupted effector. Recent evidence in Rac1 null mouse embryonic fibroblasts has shown that these cells are capable of migrating towards PDGF (30). This suggests that other signaling pathways downstream of PDGF receptors can also induce migration, but no specific signaling pathway was identified to explain the ability to bypass the Rac1 activity. Our data also suggests that the rapamycin sensitive mTORC1 complex also plays a role in migration as rapamycin treatment rendered cells incapable of migration towards PDGF. Taken together our data demonstrates a specific requirement for PI3K in PDGF receptor migration of a sclerotome-derived population. It is interesting that the deletion of PDGFRα lead to a slightly more severe vertebral arch phenotype.

This suggests that while PI3K may be a key signaling pathway driving migration, either other pathways are also involved in migration promotion or this cell population may also rely on PDGF signaling for proliferation. Using both the signaling point mutant and imatinib mesylate treatment we show that disruption of PDGFRα signaling results in spina bifida. Because disruption of PDGF receptor signaling has been proposed for treatment of several human pathologies, concern should be placed on effects that these drugs could have on fetuses.

Materials and Methods

In ovo chick studies

Fertilized White Leghorn eggs were obtained from the Texas A&M Poultry Science Department (College Station, TX), incubated at 37°C, then opened and staged at 2-3 days of development. Imatinib (a kind gift from R. Ilaria) in DMSO or vehicle were applied by bath application of 500 ml to developing embryos at HH stage 14-17. Openings were sealed with tape and allowed to develop to day 10 (HH stage 36). Embryos were removed from egg and frozen-embedded for histological sectioning. Serial sections (10 um, Safranin O stained) through the upper sacral, entire lumbar, and lower thoracic region were analyzed for the presence of chondrocytes (marked by red staining) dorsal to the neural tube, completing closure of the vertebral arch. Images represent the most advanced arch progression in affected vertebrae. Closed sacral and thoracic vertebrae were observed in all samples, drug treated and control. We analyzed 2 vehicle treated embryos, and 4 each of 25 mM and 50 mM Imatinib treated embryos.

Mice

The mutant and Cre alleles used in these experiments were: *PDGFRα*^{F2} (15), *PDGFRα*^{GFP} (20), *PDGFRα*^{fl} (21), Twist2^{Cre} (24), and *Col2a1-Cre*^{Tg} (22). The Twist2^{Cre} line was kindly provided by E. Olson. The *Col2a1-Cre*^{Tg} mice were kindly provided by G. Karsenty. Embryos possessing a tissue specific deletion of

the PDGFRα were generated by crossing males (PDGFRα$^{fl/+}$; Cre^{+}) to females homozygous for the PDGFRα$^{fl/fl}$.

Histological procedures and skeletal staining

For H&E and Safranin-O staining embryos were fixed in 4% paraformaldehyde at 4°C overnight, embedded in paraffin, sectioned at a thickness of 7 μm, and stained according to standard procedures. Skeletal preparations were performed according to (31). For RNA in situ analysis and green fluorescent protein (GFP) expression embryos were fixed in 4% PFA overnight, saturated in 10% sucrose at 4°C overnight, embedded in OCT, and sectioned at 14 μm or 10 mm, respectively. In situ analyses were performed as previously described (32). For BrdU analysis pregnant females were injected with 10 mg BrdU (Sigma) per gram of body weight one hour prior to sacrifice. Embryos were fixed and sectioned as described above. BrdU was detected by anti-BrdU (Becton Dickinson) primary antibody (1:50 dilution in block). Proliferation index was determined by counting BrdU positive and negative cells located in the region dorsal to the neural tube (demarcated by a box) in 3 sections for each genotype. Nuclei were detected by hematoxylin-QS counterstain (Vecstastain). [n=1 embryo for each genotype at each time point]. TUNEL analysis was performed by standard procedures using

biotinylated-14-dATP and detected using the strepavidin-HRP and DAB (Vectastain) kits.

Cell culture and migration anaylsis

Mesenchymal cells were isolated from the thoracic and lumbar regions of E13.5 embryos by removing surface ectoderm, neural tube, dorsal root ganglia, and vertebral column components. Remaining tissue was rinsed extensively with PBS and dispase treated (0.5 mg/ml for 10 minutes at 37°C) to form a single cell suspension. Single cell suspension was rinsed with PBS then plated. Cultures containing PDGFRα^{GFP} alleles were scored for GFP-expression as a marker of PDGFRα-expression. Passage 1 cultures were 90% (+/- 3%) GFP-positive (n=4). Passage 4 cultures were 89% (+/- 4%) GFP-positive (n=5). Marker analysis (Twist2 for dermatome and dermis, Col2a1 and Scleraxis for sclerotome and chondrocytes) was performed by RT-PCR to confirm cell culture identity and purity. Cultures were positive for Twist2, negative for Col2a1 and Scleraxis. RNA was extracted by Trizol (Invitrogen) and cDNA was generated using PowerScript Reverse Transcriptase (Clontech). Primers for RT-PCR: Twist2, For CAGAGCGACGAGATGGACAATAAG and Rev GGTTGGTCTTGTGTTTCCTCAGG; Col2a1, For TATGGAAGCCCTCATCTTGCCG and Rev TCTTTTCTCCCTTGTCACCACG; Scleraxis, For

T T C T C A C C T G G G C A A T G T G C and Rev AGTGTTCGGCTGCTTAGAGTCAAG. Cells were maintained in DMEM with 10% serum and experiments were performed between passages 1-5. PDGF ligands were obtained from R&D Systems.

For migration analysis, primary cells in single suspension were plated in triplicate at a density of $4x10^4$ cells per well in a 96-well chemotaxis chamber (NeuroProbe Inc.), on a filter (8 um pore size, PVP-free) pre-treated for 1 hour with 10ug/ml rat tail collagen. Chamber was incubated at 37°C for 6 hours. Cells were fixed with 4% PFA for 15 minutes, then rinsed with PBS. Unmigrated cells were scraped away. Cells remaining on the filter were stained with DAPI and filter strips were mounted on slides. For each well, three 20X fields-of-view were scored for migrated GFP-positive cells. The migration assay was performed twice in triplicate. For migration analysis using drug inhibition, wild type cells were treated with rapamycin (20 ng/ml) or an equal volume of vehicle (90% ethanol, 10% Tween-20) for 48 hours prior to plating in migration chamber in media containing rapamycin (20 ng/ml) or vehicle. Otherwise, migration analysis was performed as described above.

For western blot analysis, cells were starved (in DMEM with 0.1% serum) for 48 hours, then stimulated with 10 ng/ml PDGF-AA or 10% serum for 5 minutes. Whole cell lysates were run on 7.5% SDS-PAGE and transferred to PVD membranes. Antibodies: cytoskeletal actin loading control [Novus, 1:5,000],

AKT-p(Ser473) [Cell Signaling, 1:1,000], AKT [Cell Signaling, 1:1,000[, FAK [Cell Signaling, 1:1,000], FAK-p(Tyr576/577) [Cell Signaling, 1:1,000], MAPK-p(P44,42) [Cell Signaling, 1:5,000], MAPK [Cell Signaling, 1:2,500], PAK1 [Cell Signaling, 1:1,000], PAK1-p(Ser199/204) [Cell Signaling, 1:1,000], PAK1-p(Thr423) [Cell Signaling, 1:1000], PDGFRα [Santa Cruz, 1:333], p70S6K-p(Thr389) [Cell Signaling, 1:1,000], and p70S6K [Cell Signaling, 1:1000].

Micromass culture analysis

Limb buds isolated from E11.5 embryos were rinsed extensively with PBS, dispase treated (1 U/ml for 30 minutes at 37°C), rinsed, and dispersed to make a single cell suspension. Cells were plated in 25 μl droplets at a density of $1x10^7$ cells/ml of basal media (DMEM with 2% serum) and incubated at 37°C for 1 hour. Growth factor and conditioned media treatments were performed in triplicate. Conditioned media was harvested from cells cultured at density of $5x10^5$ cells per well 3 ml of DMEM with 10% serum for 24 hours. Micromass cultures were fixed in ethanol after 5 or 7 days of culture and chondrocyte nodules were stained with 1% Alcian blue. Stained cultures were rinsed with 3% acetic acid to remove excess stain. Alcian blue was extracted with 300 μl 4 M guanidine-HCl. Extracted Alcian blue was measured by OD_{600} (Amersham Biosciences GeneQuant pro spectrophotometer). Each experiment was repeated 3 times for the 4-5 day assay and 2 times for 7 day assay.

Figures

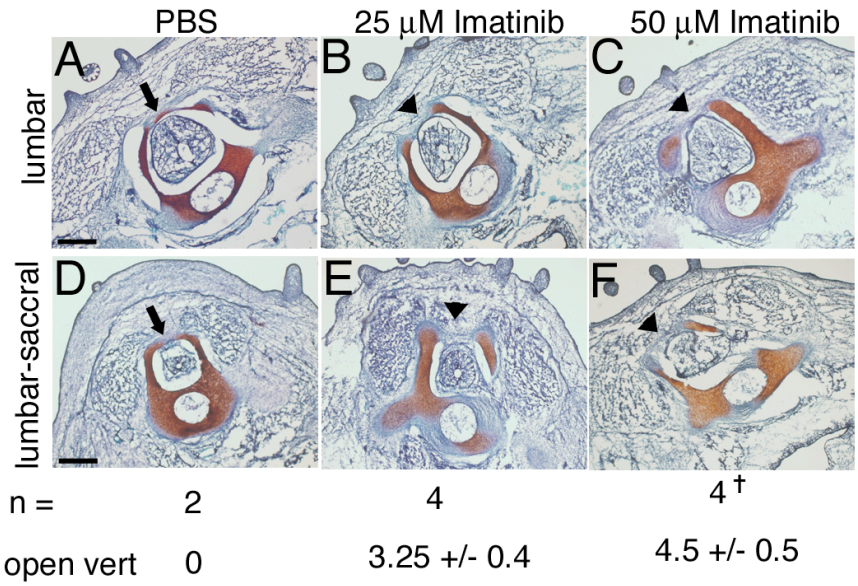

Figure 2-1. Induction of spina bifida by imatinib-mesylate
Representative saffranin-O stained transverse sections through the lumbar and lumbar-saccral regions of chick embryos (HH stage 36). (A, D) vehicle treated, (B, E) 25 mM, and (C, F) 50 mM imatinib-mesylate treated. The lamina failed to form across the dorsal midline in imatinib-treated embryos, resulting in spina bifida. Images show the most advanced arch formation found in serial sections of each treatment group. 2-4 embryos were examined in each group. Open vertebrae were quantified by analysis of Safranin O stained continuous serial sections through the sacral, lumbar, and lower thoracic regions. Scale bars = 200 mm. †Two out of four embryos treated with 50mM imatinib-mesylate also exhibited failure of ventral closure.

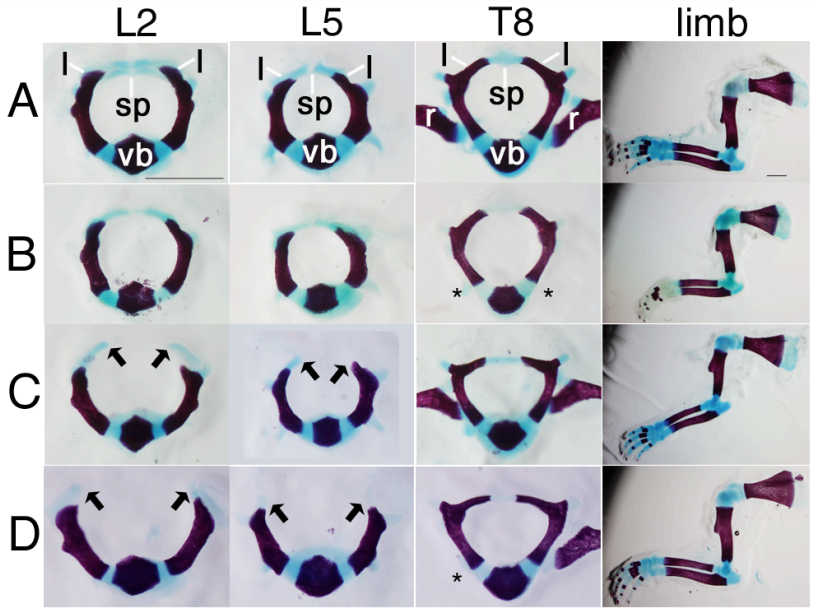

Figure 2-2. Spina bifida in PDGFRα mutant embryos
Skeletal preparations of E18.5 embryos display defects in lumbar vertebrae formation. (A) control, (B) PDGFRα^{CKO} (C) PDGFRα$^{PI3K/PI3K}$, and (D) PDGFRα^{TKO}. The vertebral arches form normally in A and B but fail to progress in C and D. Data representative of skeletal preparations performed on E18.5 and P1 embryos: wild type (n=10); PDGFRα^{CKO} (n=4); PDGFRα$^{PI3K/PI3K}$ (n=10); and PDGFRα^{TKO} (n=9). Vertebral arch development of the thoracic vertebrae and limbs was normal in all embryos. Scale bars = 1 mm. Arrows point to most advanced formation of lamina in mutants. Asterisks denote location of bones lost during dissection. (sp) spinous process; (l) lamina; (vb) vertebral body; and (r) ribs.

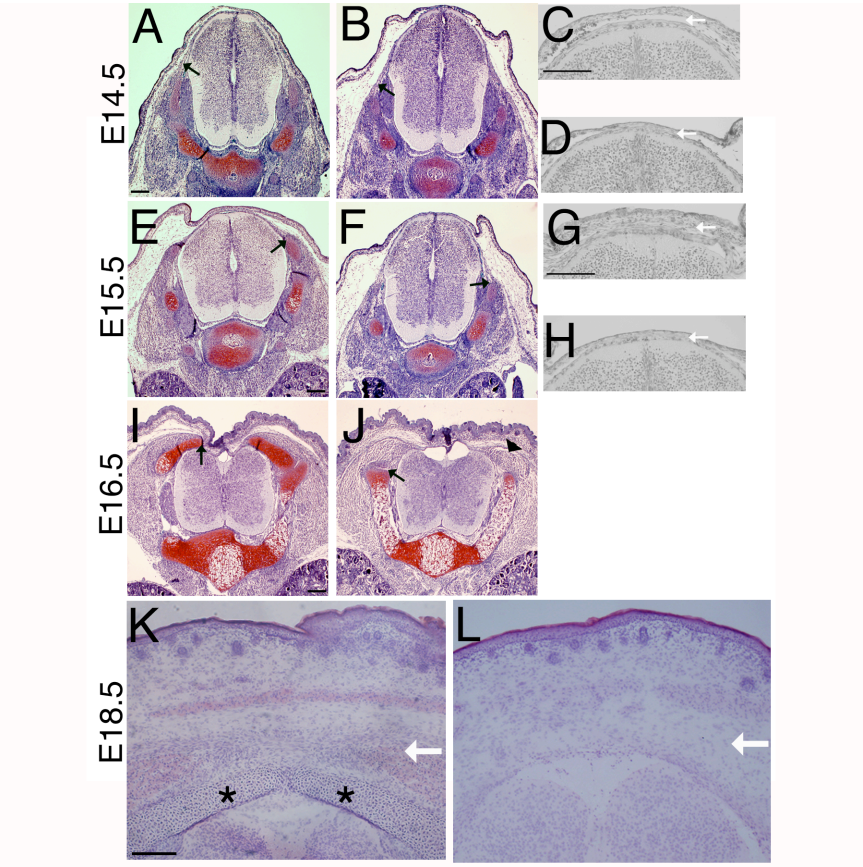

Figure 2-3. Timing of vertebral arch defect.

(**A,B,E,F,I,J**) Safranin-O stained transverse sections through lumbar vertebrae. By E15.5, the development of the vertebral arch in the mutant lags behind that of the wt littermate, and failure of the vertebral arch to fully form is observed at E16.5. Sections are representative of the furthest progression of the vertebral arch in the lumbar region at each time-point, and arrows denote furthest progression of vertebral arch. Arrowhead in **(J)** indicates undifferentiated mesenchyme. (**C,D,G,H**) The number of cells present dorsal to the neural tube is reduced in PDGFRα$^{PI3K/PI3K}$ mutants **(D,H)** compared to littermate controls (**C,G)** as early as E14.5. The loss of the cell population was more pronounced at E15.5. **(G,H)**. White arrows point to dorsal cell population. H&E stained sections from E18.5 wild type **(K)** and PDGFRα^{TKO} **(L)** show missing vertebral arch and overlying dorsal cells. Asterisks mark the vertebral arch. Scale bars = 100μm.

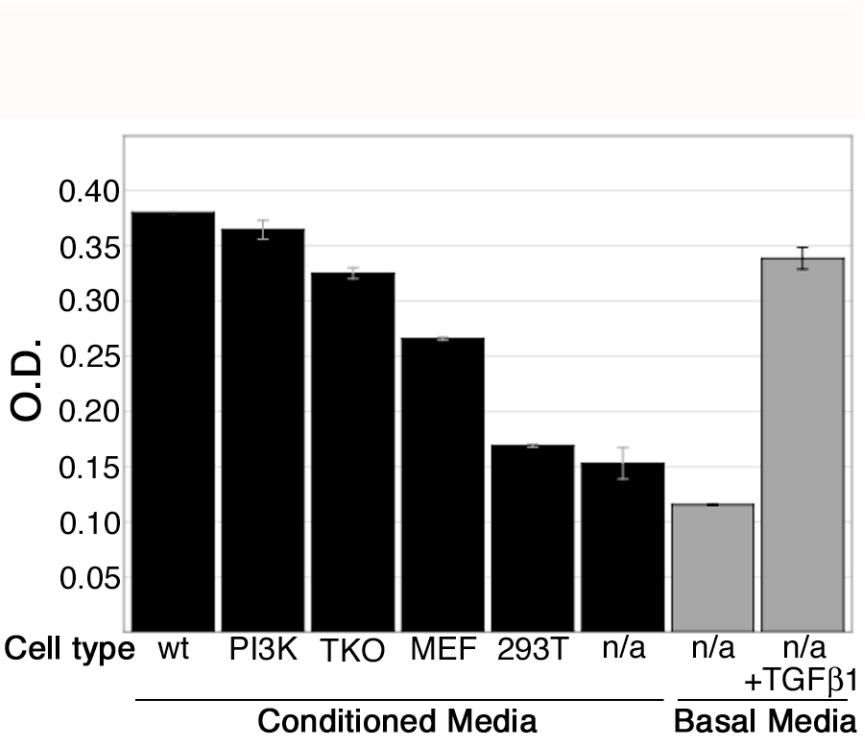

Figure 2-4. Cells of the adjacent meshenchyme are capable of inducing chondrogenesis.

Conditioned media from wt, PDGFRα mutant, and MEF cells promoted chondrogenesis of micromass cultures, while conditioned media from HEK293T cells did not. Note that chondrogenesis occurred regardless of the genotype of the cultured mesenchyme cells, indicating that PDGF signaling is not required for secretion of the chondrogenic factor. Black bars indicated media containing 10% serum, grey bars indicate media containing 2% serum.

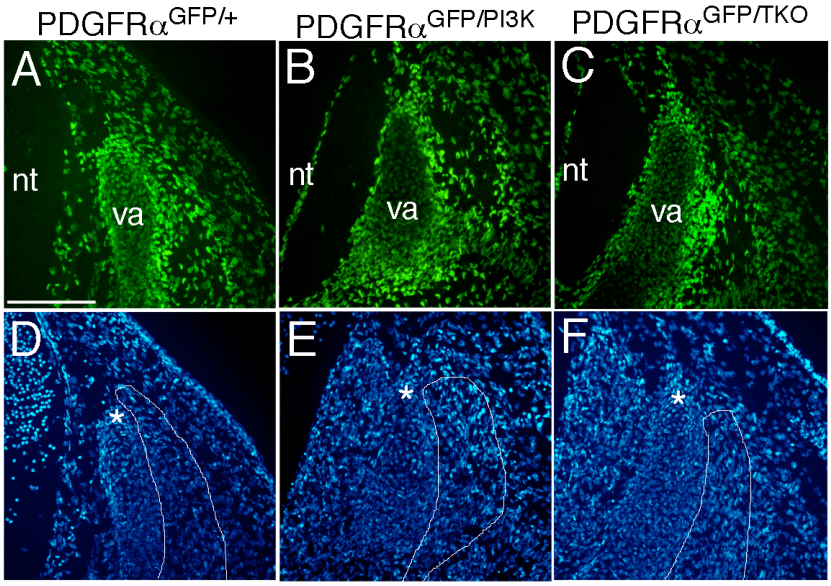

Figure 2-5. Loss of PDGFRα-PI3kinase signaling results in defective migration
PDGFRα-expressing cells (as detected by PDGFRα^{GFP}) are present in the perichondrium and in the mesenchyme surrounding the vertebral arch (**A,B,C**). Heterozygote control section is at the level of the perichondrium and therefore displays more PDGFRα-positive chondrocytes. Note that the PDGFRα-positive mesenchyme adjacent to the vertebral arch extends just past the tip of the arch in the heterozyote control (**B**), but has failed to advance in the mutants (**B,C**). Sections are representative of furthest advancement of the vertebral arch and adjacent mesenchyme population in two embryos of each genotype. (nt) neural tube, (va) vertebral arch. Asterisk denotes tip of vertebral arch, white line outlines PDGFRα^{GFP}-expressing mesenchyme. Scale bar = 100μm.

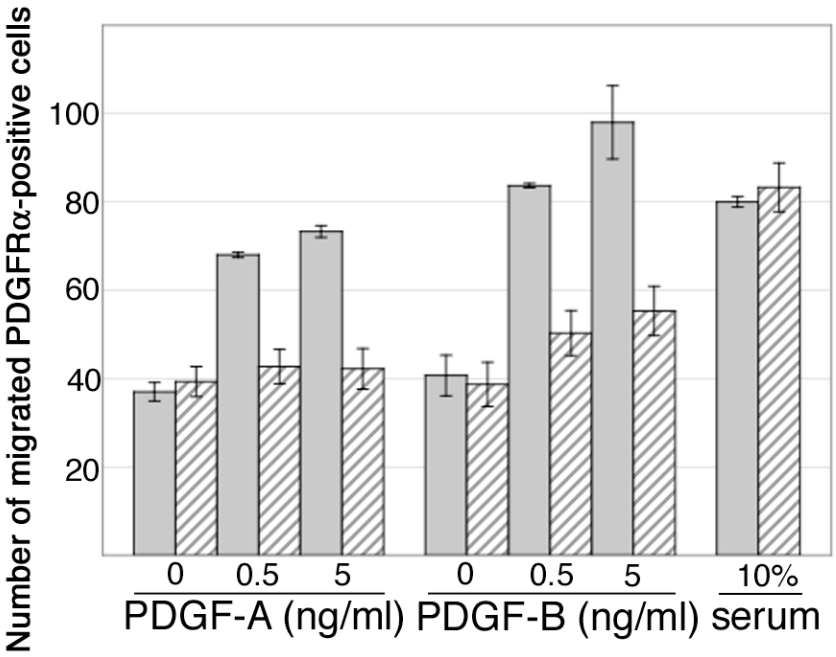

Figure 2-6. PDGFRα$^{PI3K/PI3K}$ cells fail to migrate towards PDGF-A ligand
In vitro migration assay on heterozygous cells (gray bars) migrated in a dose-dependent manner in response to PDGF-A and PDGF-B ligands, while mutant cells (striped bars) were unable to migrate in response to PDGF-A and showed a decreased response to PDGF-B. Both genotypes were able to migrate in response to 10% serum. This experiment is representative of 2 independent experiments.

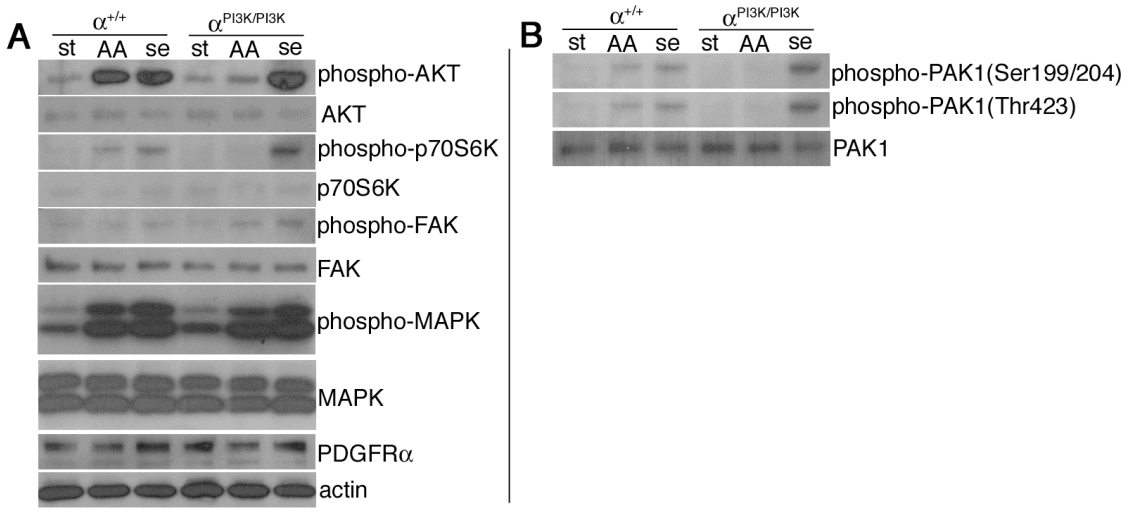

Figure 2-7. Reduced p70S6K and PAK1 signaling in PDGFRα$^{PI3K/PI3K}$ cells
(A) Whole cell lysates from cultured mesenchyme show decreased phosphorylation of p70S6 kinase and Akt in mutant cells in response to PDGF stimulation, while phosphorylation of FAK and MAPK are unaffected. **(B)** PAK1 phosphorylation is decreased in mutant cells at both the autophosphorylation sites (Ser199/204) as well as the PKD1 site (Thr423). Stimulation conditions: starved (st), 10 ng/ml PDGF-AA (AA), 10% serum (se). Blots are representative of 3 independent experiments.

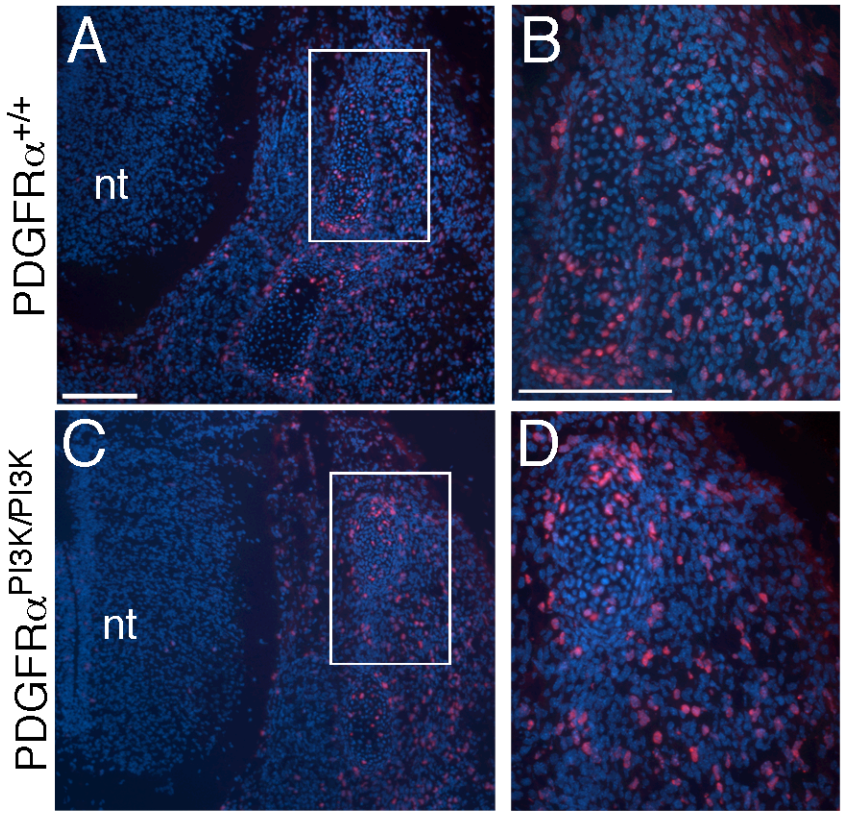

Figure 2-8. No alteration in proliferation at E14.5
BrdU (red) incoporation in the chondrocytes and mesenchyme of PDGFRα$^{PI3K/PI3K}$ **(C,D)** and littermate control **(A,B)** embryos reveal no differences in proliferation. (**B,D**) show view of cells within white boxes in (**A,C**). nt = neural tube.

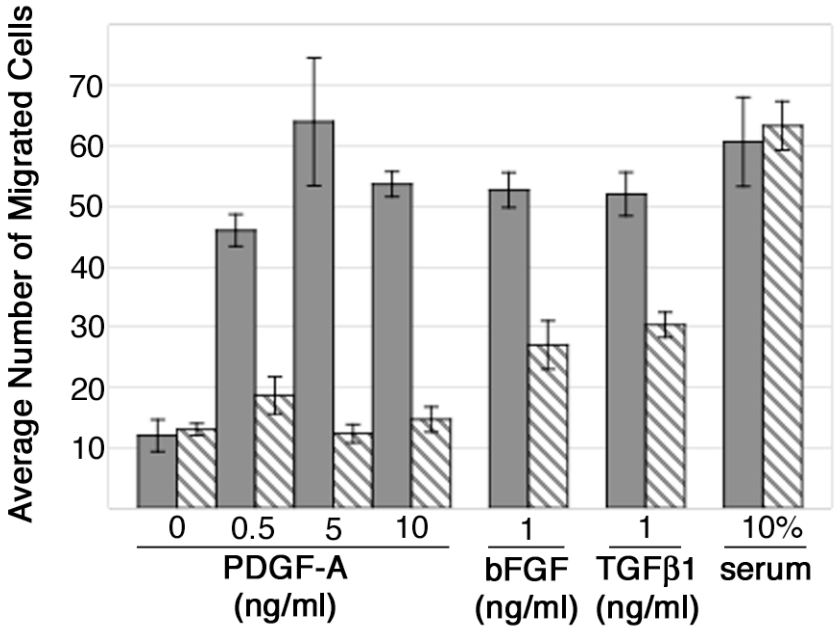

Figure 2-9. Rapamycin inhibits migration of primary mesenchyme cells.
Treatment with rapamycin inhibits the ability of wild type primary mesenchyme cells to migrate toward PDGF, FGF, and TGFβ1 ligand, but not serum. Striped bars indicate treatment with rapamycin, solid bars indicate treatment with vehicle. Data is representative of two experiments performed in triplicate.

References

1. Nagel, M., Tahinci, E., Symes, K., & Winklbauer, R. (2004) *Development* **131,** 2727-2736.
2. Duchek, P., Somogyi, K., Jekely, G., Beccari, S., & Rorth, P. (2001) *Cell* **107,** 17-26.
3. Wennstrom, S., Hawkins, P., Cooke, F., Hara, K., Yonezawa, K., Kasuga, M., Jackson, T., Claesson-Welsh, L., & Stephens, L. (1994) *Curr Biol* **4,** 385-393.
4. Kundra, V., Escobedo, J. A., Kazlauskas, A., Kim, H. K., Rhee, S. G., Williams, L. T., & Zetter, B. R. (1994) *Nature* **367,** 474-476.
5. Wennstrom, S., Siegbahn, A., Yokote, K., Arvidsson, A. K., Heldin, C. H., Mori, S., & Claesson-Welsh, L. (1994) *Oncogene* **9,** 651-660.
6. Heuchel, R., Berg, A., Tallquist, M., Ahlen, K., Reed, R. K., Rubin, K., Claesson-Welsh, L., Heldin, C. H., & Soriano, P. (1999) *Proc Natl Acad Sci U S A* **96,** 11410-11415.
7. Boyle, S. N., Michaud, G. A., Schweitzer, B., Predki, P. F., & Koleske, A. J. (2007) *Curr Biol* **17,** 445-451.
8. Ferns, G. A., Sprugel, K. H., Seifert, R. A., Bowen-Pope, D. F., Kelly, J. D., Murray, M., Raines, E. W., & Ross, R. (1990) *Growth Factors* **3,** 315-324.
9. Hosang, M., Rouge, M., Wipf, B., Eggimann, B., Kaufmann, F., & Hunziker, W. (1989) *J Cell Physiol* **140,** 558-564.
10. Matsui, T., Pierce, J. H., Fleming, T. P., Greenberger, J. S., LaRochelle, W. J., Ruggiero, M., & Aaronson, S. A. (1989) *Proc Natl Acad Sci U S A* **86,** 8314-8318.
11. Eriksson, A., Siegbahn, A., Westermark, B., Heldin, C. H., & Claesson-Welsh, L. (1992) *Embo J* **11,** 543-550.
12. Stedman, T. L. (2000) (Lippincott Williams & Wlikins, Philadelphia).
13. Juriloff, D. M. & Harris, M. J. (2000) *Hum Mol Genet* **9,** 993-1000.
14. Payne, J., Shibasaki, F., & Mercola, M. (1997) *Dev Dyn* **209,** 105-116.
15. Klinghoffer, R. A., Hamilton, T. G., Hoch, R., & Soriano, P. (2002) *Dev Cell* **2,** 103-113.
16. Soriano, P. (1997) *Development* **124,** 2691-2700.
17. Buchdunger, E., O'Reilly, T., & Wood, J. (2002) *Eur J Cancer* **38 Suppl 5,** S28-36.
18. Orr-Urtreger, A. & Lonai, P. (1992) *Development* **115,** 1045-1058.
19. Takakura, N., Yoshida, H., Ogura, Y., Kataoka, H., Nishikawa, S., & Nishikawa, S. (1997) *J Histochem Cytochem* **45,** 883-893.

20. Hamilton, T. G., Klinghoffer, R. A., Corrin, P. D., & Soriano, P. (2003) *Mol Cell Biol* **23,** 4013-4025.
21. Tallquist, M. D. & Soriano, P. (2003) *Development* **130,** 507-518.
22. Ovchinnikov, D. A., Deng, J. M., Ogunrinu, G., & Behringer, R. R. (2000) *Genesis* **26,** 145-146.
23. Yoon, B. S., Ovchinnikov, D. A., Yoshii, I., Mishina, Y., Behringer, R. R., & Lyons, K. M. (2005) *Proc Natl Acad Sci U S A* **102,** 5062-5067.
24. Yu, K., Xu, J., Liu, Z., Sosic, D., Shao, J., Olson, E. N., Towler, D. A., & Ornitz, D. M. (2003) *Development* **130,** 3063-3074.
25. Boyd, L. M., Chen, J., Kraus, V. B., & Setton, L. A. (2004) *Spine* **29,** 2217-2222.
26. Ronnstrand, L. & Heldin, C. H. (2001) *Int J Cancer* **91,** 757-762.
27. Tanski, W. J., Nicholl, S. M., Kim, D., Fegley, A. J., Roztocil, E., & Davies, M. G. (2005) *J Vasc Surg* **41,** 91-98.
28. Dharmawardhane, S., Sanders, L. C., Martin, S. S., Daniels, R. H., & Bokoch, G. M. (1997) *J Cell Biol* **138,** 1265-1278.
29. Sells, M. A., Knaus, U. G., Bagrodia, S., Ambrose, D. M., Bokoch, G. M., & Chernoff, J. (1997) *Curr Biol* **7,** 202-210.
30. Vidali, L., Chen, F., Cicchetti, G., Ohta, Y., & Kwiatkowski, D. J. (2006) *Mol Biol Cell* **17,** 2377-2390.
31. (1994) *Manipulating the Mouse Embryo* (Cold Spring Harbor Press, Cold Spring Harbor, NY).
32. Wilkinson, D. G. (1992) *Whole mount in situ hybridization to vertebrate embryos* (IRL Press, Oxford).

CHAPTER THREE

PDGF Receptor alpha Deficient Dermis Exhibits
Fraser Syndrome-like Epidermal Blistering

Abstract

Previous studies have demonstrated an essential role for platelet-derived growth factor receptor α (PDGFRα) during embryonic development, in processes such as mesenchymal cell proliferation and neural crest cell migration. Although platelet-derived growth factor (PDGF) signaling is generally considered to be a key component in extracellular matrix biology, evidence supporting this role during embryogenesis is lacking. In this report, we show that PDGFRα signaling in the dermis is required for normal dermal epidermal junction (DEJ) formation. Embryos with a deletion of PDGFRα in dermis formed subepidermal blisters reminiscent of defects observed in Fraser syndrome, a human disorder characterized by skin blistering. This defect was not caused by a failure to form dermis but by a failure in dermis extracellular matrix (ECM) maintenance. PDGFRα deficient dermis exhibited normal deposition of many matrix molecules but contained a progressive loss of FREM1 localization to the basement membrane. Frem1 is secreted by the dermis and believed to be an essential component of the DEJ. Our results demonstrate that PDGFRα-mediated signaling is required in the dermis to maintain dermal-epidermal adhesion.

Introduction

Anchorage of the epidermis to the underlying dermis is an essential process in skin development. Blistering of the fetal epidermis is a feature of Fraser syndrome, a disorder also characterized by cryptophthalmos, syndactyly and renal agenesis (1-3). Five mouse blebbing mutants (*blebbed*, *fetal hematoma, eye blebs, head blebs,* and *myelencephalic blebs*) serve as animal models for Fraser syndrome (4, 5). Genetic mapping of four of the blebbing loci in mice has demonstrated several new proteins required for embryonic dermal-epidermal adhesion. The FRAS/FREM gene family, Fras1, Frem1, and Frem2, are extracellular matrix (ECM) components that contribute to dermal-epidermal junctions (DEJ), and Grip 1 is a PDZ adaptor protein that interacts physically with Fras1 (1, 3, 6-9). These and other genetic studies have demonstrated a critical role for these structural proteins in the epidermis for maintenance of adhesion, but less is known about the contribution of proteins from the dermis in these interactions.

PDGFRα is a receptor tyrosine kinase that has been implicated in numerous cellular functions, including proliferation, migration and survival (reviewed by (10)). In many tissues during organogenesis PDGFRα is expressed by the mesenchyme, and its ligands, PDGFA and PDGFC, are secreted by the overlying epithelium (11-14). This same signaling paradigm has been reported in the developing skin, where PDGFRα is expressed in the dermis and the ligands in the epidermis. Further support for the role of the PDGFRα in the dermis is the

presence of multiple epidermal blebs and dermal hypoplasia in *Pdgfrα* null animals (15). In addition, mice lacking PDGFA have dermal hypoplasia and hair abnormalities (12), while PDGFC deficient embryos have hemorrhagic sub-epidermal blebs on the face**,** limbs, and palate analogous to PDGFRα deficiency (16). The molecular basis of skin blistering in embryos with disrupted PDGFRα signaling is unknown, although various mechanisms have been proposed, including edema, reduced dermal proliferation, and loss of anchoring fibrils (12, 15, 16).

In this report we provide the first evidence that signaling by the PDGFRα in the dermis is essential for maintenance of dermal-epidermal adhesion. We establish that PDGFRα-deficient embryos have dermal-epidermal cleavage below the level of the lamina densa, reminiscent of the phenotype seen in the mouse blebbing mutants. Next, we demonstrate that PDGFRα-deficient embryonic dermis has significantly reduced levels of collagen type VI, a putative extracellular ligand of the Fraser syndrome ECM associated proteins. Finally, we demonstrate that loss of PDGFRα in the dermis leads to aberrant patterns of Frem1 localization. These data demonstrate that PDGFRα signaling is required in the dermis to maintain dermal-epidermal adhesion.

Results

Loss of PDGFRα results in epidermal blistering

Mutations in PDGFRα signaling components, including *Pdgfa*, *Pdgfc*, and *Pdgfrα*, lead to multiple defects in the skin including blistering, dermal fibroblast hypoplasia, and hair loss (12, 15-19). Reduced proliferation of dermal progenitors in *Pdgfa* null animals has been suggested as a cause of blistering (12), but we have observed blistering with no apparent loss of dermal cell populations in embryos expressing PDGFRα hypomorphic and null alleles (17, 20). In the limbs of PDGFRα null embryos that survived until E13.5, we observed no dermal hypoplasia but consistently found epidermal blistering (Fig. 1A, F-G). This observation led us to explore the possibility that blebbing induced by lack of PDGFRα signaling was not caused directly by dermal hypoplasia.

Most *Pdgfrα*$^{-/-}$ embryos exhibit surface ectoderm blistering on the head and body as early as E9.5 (18, 21-23), but often these embryos die before E10.5, likely due to placental abnormalities (15, 24). All surviving *Pdgfrα*$^{-/-}$ embryos had characteristic, sometimes symmetric blebbing along the dorsal-lateral trunk, the midline of the face, the branchial arches, and on the dorsi of the limbs (Fig. 1A). To circumvent extraembryonic pathology, we generated embryos with epiblast-specific deletion of *Pdgfrα* using a Cre recombinase driven by the *Meox2* promoter (*Meox2*^{Cre}) (25) and a *PDGFRα loxP* flanked (*PDGFRα*^{fl}) allele (20).

These "*Meox2*^{Cre} conditional" embryos recapitulated the blistering phenotype seen in *Pdgfrα*$^{-/-}$ embryos (Fig. 1B-C), yet, circumvented the early lethality observed for *Pdgfrα* null embryos. Western blotting confirmed that PDGFRα protein was not detectable in *Meox2*^{Cre} conditional embryonic tissue (Fig. 1H), indicating widespread deletion of the floxed allele in the embryo proper as previously reported (26-28). The blistering in the limbs of *Meox2*^{Cre} conditional embryos was indistinguishable from that seen in the *Pdgfrα*$^{-/-}$ embryo limbs.

Proliferation and survival are not affected in embryonic dermis

We sought to examine the mechanism of epidermal blebbing in the absence of PDGFRα signaling. It has been reported that *Pdgfrα*$^{-/-}$ and *Pdgfa*$^{-/-}$*;Pdgfc*$^{-/-}$ embryos have significant subcutaneous edema and mesenchymal hypoplasia of the trunk, neck and head, and this was a potential etiology of epidermal blebs (15, 16, 18, 23). We therefore focused our studies on the limbs of *Meox2*^{Cre} conditional embryos because gross development of the limbs was normal, yet epidermal blebs were frequent. Because PDGFRα signaling has been implicated in proliferation of the postnatal dermis, craniofacial mesenchyme, and the somites (12, 15, 20), we compared the levels of dermis proliferation (phosphohistone-H3^{+} cells, PH3) in the limbs of *Meox2*^{Cre} conditional and control littermates. At time points E11.5 and E15.5 we observed no differences in the number of cells that were PH3^{+} (data not shown). To complement our in vivo

analysis of proliferation, we examined the effects of PDGF receptor stimulation on primary dermal fibroblasts (PDFs). PDFs exhibited only minimal proliferation in response to treatment with PDGFAA. In contrast, PDFs proliferated robustly upon stimulation with 10% FBS or FGF (Table I). These results were in agreement with previous reports that demonstrated that PDGFRα stimulation did not promote proliferation of dermal fibroblasts (29-31) and demonstrated that dermal hypoplasia did not account for the limb blistering.

PDGFRα expression in dermis

To confirm previous reports that have documented PDGFRα expression in the sub-epidermal mesenchyme (12, 23) we used a *Pdgfrα*$^{GFP/+}$ mouse line. This mouse has GFP inserted at the *Pdgfrα* locus, and GFP can be used to trace *Pdgfrα* expression (24). We detected GFP expression in a majority of the cells in the dermis. Interestingly, equivalent numbers of GFP positive cells were present in the mutant and control limb dermis during embryogenesis and at birth (Fig. 2 A-D). In Fig. 2B and 2D, limbs were co-stained with laminin to define the boundary between the epidermis and dermis. We also observed no reduction in the dermal layer when a limb blister was present (Fig. 2G).

Ultrastructural analysis of the skin

Transmission electron microscopy (TEM) of *Pdgfc* null embryos demonstrated blistering with cleavage below the basement membrane and a reduction of collagen fibrils (16). Analysis of DEJ of $Meox2^{Cre}$ conditional embryos at E15.5 demonstrated a similar cleavage below the lamina densa (Fig. 2 G-H). In addition, basement membrane structures such as hemidesmosomes and anchoring fibrils were present (Fig. 2 E-H). To better characterize the blebbing phenotype of $Meox2^{Cre}$ conditional embryos, we next determined the plane of dermal-epidermal cleavage. Examination of the basement membrane by immunofluorescent staining with antibodies against integrin α6, collagen type IV, and collagen type VII in intact $Meox2^{Cre}$ conditional skin was similar to control staining. In the presence of epidermal blebs these antigens localized to the blister roof (SI Fig. 5 and data not shown). These results demonstrated that dermal-epidermal cleavage occurred beneath the lamina densa, analogous to the ultrastructural pathology seen in Fraser syndrome and the mouse blebbing mutants (1, 6, 7, 9)}.

Production of dermal matrix by PDGFRα deficient embryos

Because PDGF stimulation of fibroblasts can induce matrix production and secretion (32, 33), we examined the expression of multiple matrix proteins in the limb skin of PDGFRα-deficient embryos. We found that collagens type I, III,

V, VII, and fibronectin were expressed and localized similarly in the dermis of control and PDGFRα-deficient limbs (Fig. 5). One matrix protein that was consistently reduced in expression was collagen type VI. In the dermis of the back and limb we observed less collagen type VI (Fig. 5H and Fig. 6). However, PDGFRα deficiency did not result in global collagen type VI loss: muscle, cartilage and trachea retained normal levels (Fig. 6).

Collagen type VI forms a microfibrillar network (34), is believed to be important for matrix organization (35), and is absent or reduced in Fras1 and Grip1 deficient basement membranes (1, 3, 8). Unlike the Fras1 and Grip1 mutants, we still observed collagen type VI staining associated with the basement membrane of *Meox2*^{Cre} conditional skin, albeit at reduced levels (Fig. 5H and Fig. 6). We next sought to determine the mechanism of dermal collagen type VI loss in *Meox2*^{Cre} conditional embryos. Because collagen type VI is an obligate heterotrimer, one possible mechanism of protein deficiency was diminished transcription of one or more of its subunits (36). We examined the transcription levels of the collagen type VI subunits in *Meox2*^{Cre} conditional limb tissue. As shown in SI Fig. 5M, mRNA levels of *COL6A1*, *COL6A2* and *COL6A3* were reduced in *Meox2*^{Cre} conditional limbs. To determine if the transcription of other collagens was also affected, we analyzed mRNA levels of other dermal collagens. As shown in SI Fig. 5N, *COL1A1*, *COL3A1* and *COL5A* mRNA levels were unaffected by a deficiency in PDGFRα expression.

Phenotype of embryos with dermal deletion of PDGFRα

While the *Meox2*^{Cre} conditional embryos provided some initial insights into the blistering phenotype, we were concerned that loss of PDGFRα from the vasculature could be exacerbating the dermal phenotype by increasing the amount of edema. To determine the effects of loss of PDGFRα specifically in the dermis, we used the *Twist2*^{Cre} mouse line. Twist2 is expressed in condensing mesenchyme, osteoblasts, and the dermis (37). Fig. 3A shows the distribution of Cre activity using the *ROSA26R* reporter strain of mouse to trace Cre expression. While the dermis demonstrated Cre activity based upon β-galactosidase expression, Cre activity in the epidermis was not observed. Using the *Twist2*^{Cre} and the *PDGFRα*^{fl} allele mice, we generated embryos which lacked *PDGFRα* in the dermis, (*Twist2*^{Cre} conditional), and the resulting offspring exhibited a blistering phenotype very similar to the *Meox2*^{Cre} conditional animals but had reduced occurrence of edema (Fig. 3B and 3F). Although many of the PDGFRα dependent cell populations were normal, these animals still exhibited spina bifida and cleft palate and death at birth. The *Twist2*^{Cre} conditional embryos exhibited blistering on the limbs, along the dorsal midline, in the head, and occasionally over the eye. The *Twist2*^{Cre} conditional embryos have a dermal cell layer that is comparable to wild type embryos, but the cells appear disorganized and the hair follicles immature (Fig. 3 C, D). In contrast to most of the bleb gene mutant

animals, our embryos did not exhibit syndactyly or kidney agenesis although an eye defect was observed. In two out of six mice found at birth, we observed micropthalmia or anopthalmia similar to the phenotype reported in the *my*^{F11} mouse line (38) (Fig 3 G-J). This failure in neuroretina formation may have been caused by the early blistering over the eye, and failure of the ectoderm to signal to the developing optic vesicle (39).

By TEM there appeared to be a slightly reduced collagen fibril content, but this varied between the sections that were examined (Fig. 2I-L). When we determined the collagen matrix levels in the *Twist2*^{Cre} conditional embryos, we observed normal levels of type IV and VI collagen (Fig. 4). These results suggested that the type VI collagen reduction that we observed in the *Meox2*^{Cre} conditional and PDGFRα null embryos was caused by the early deletion of the PDGFRα.

Frem1 localization is disrupted in PDGFRα dorsal dermis

Because the phenotype of the PDGFRα deficient dermis was similar to the blistering observed in the Grip1, Fras1, and Frem 1 and 2 (40), we examined the composition of the basement membrane in our mutant skin. Previously, analysis of the Frem family, Grip1, and Fras1 protein expression has suggested that these proteins exist in a complex at the basement membrane, and loss of any one of these proteins results in blister formation and destabilization of the complex at the

basement membrane (41). To determine if any of these proteins were disrupted in the PDGFRα mutant skin we analyzed the dorsal dermis by immunohistochemistry (Fig. 4). Most proteins that we examined were expressed at similar levels in control and *Twist2*^{Cre} conditional tissues, and many of the components of the basement membrane were correctly localized. Only Frem1 and Frem 2 showed a different expression pattern. Although Frem1 protein was detected in the dermis and other tissues, Frem1 was not concentrated at the basement membrane. In multiple areas along the dorsal skin basement membrane we observed significantly reduced or absent Frem1 (Fig 4). Examination of postnatal day 1 (P1) mice demonstrated a similar loss of Frem1 from the basement membrane. In addition, Frem1 presence in the hair follicles was also reduced, and Frem2 expression was decreased throughout the epidermis. To determine if the loss of Frem1 localization occurred at earlier stages of development we examined E16.5 dorsal dermis and found that while slightly reduced compared to littermate controls, Frem1 staining was still present in the basement membrane of *Twist2*^{Cre} conditional embryos (Fig 4).

We next determined if PDGFRα is necessary for expression of the established bleb genes; *Grip1*, *Fras1*, *Frem1*, and *Frem2* (1, 3, 6-9). Most of the bleb genes are expressed at high levels in differentiating epidermis that is interacting with underlying mesenchyme (40). Frem1 is an exception because it is expressed by the dermis (7). We examined limb tissue from the *Meox2*^{Cre}

conditional embryos and dorsal dermis of *Twist2*^{Cre} conditional embryos for bleb family gene expression. The transcription of *Grip1*, *Fras1, Frem1,* and *Frem2* was not reduced in PDGFRα-deficient dermis (Fig. 4). These data suggested that transcription of the bleb genes was not affected by PDGFRα-deficiency. The loss of Frem1 protein localization but normal transcript expression was similar to loss of basement membrane and matrix components observed in embryos lacking epidermal Grip1 or Fras1 (3, 8). Taken together these data demonstrated that loss of PDGFRα signaling in the dermis did not disrupt dermal fibroblast formation but was required for maintenance of the DEJ.

Discussion

In this report we demonstrate that PDGFRα signaling is required for dermal-epidermal adhesion in the embryo. Like the mouse blebbing mutants, PDGFRα-deficient embryos and PDGFC-deficient embryos have characteristic hemorrhagic blebbing on the face, head and limbs, with dermal-epidermal separation below the level of the basement membrane ((15, 16), this report). Despite these phenotypic similarities, transcription of the known bleb genes was not affected in PDGFRα-deficient embryos. It is also worth noting that extracutaneous features of the bleb gene mutations (renal agenesis and syndactyly) were not manifestations of PDGFRα-deficiency (10, 15).

Pdgfa$^{-/-}$ mice exhibit dermal hypoplasia and hair loss with a marked decrease in proliferation of dermal papillae and mesenchyme in post-natal tissues (12). In our *Meox2*^{Cre} conditional embryos we observed mesenchymal hypoplasia in the dorsal trunk region, but in the limbs where we consistently observed subepidermal blebbing, there was no reduction in mesenchymal cells. In addition, we did not observe any dermal hypoplasia in the *Twist2*^{Cre} conditional embryos. Therefore, signaling through the PDGFRα may have two distinct outcomes; extracellular matrix regulation which affects the DEJ during embryogenesis and maintenance of dermal progenitor cell proliferation in the adult. Subepidermal blistering was also observed in the frontonasal process and lateral forehead and dorsal aspects of the spinal cord and limbs of *Pdgfc*$^{-/-}$ embryos. The blisters in

these embryos occurred in the sublamina densa and a reduction in anchoring fibrils was noted (16). This phenotype is similar to the phenotype that we describe here suggesting that PDGFC may be the ligand responsible for PDGFRα dependent matrix production during embryonic development while PDGFA may direct dermal progenitor formation. Both PDGFRα specific ligands, PDGFA and PDGFC, are expressed in the surface ectoderm as early as E9.5 and continue to be expressed in the basal epidermis past E14.5 (12, 13, 42, 43). Because PDGFC is secreted as a latent growth factor that requires proteolysis (44, 45), it may be active during tissue remodeling or in pathological situations. These features may give it unique abilities to activate the PDGFRα and explain the difference in dermis phenotypes of the ligand knockouts despite the similar expression patterns.

Although PDGF receptors have long been considered important agonists of ECM production during wound healing (46) and fibrotic disease (47), we present the first evidence for this function during embryogenesis. It is interesting that type VI collagen expression in the dermis was affected by loss of the PDGFRα, but it is unlikely that this aspect of the dermis matrix has a major function in bleb formation because we did not see the same reduction in the *Twist2*^{Cre} conditional embryos. The loss of Frem1 localization in the *Twist2*^{Cre} conditional embryos supports previous data suggesting that loss of the bleb genes at the basement membrane is indicative of detachment of the epidermis from the dermis. In Frem1 mutants, Frem2 was no longer localized to the basement

membrane (7, 41). We found that while Frem1 localization was disrupted, disruption of Frem2 localization occurred with slower kinetics. It is important to note that similar to the bleb gene mutants, we observed blistering only in specific regions of the skin, but Frem1 localization was disrupted throughout the dorsal skin. The suggested explanation for regional blistering is that it occurs only in locations were the embryonic skin may be physically agitated by rubbing or movement (7).

In summary, we have shown that PDGFRα signaling is required for dermal-epidermal adhesion in the embryo, and that PDGFRα-deficient embryos have a skin blebbing phenotype strikingly similar to that seen in patients with Fraser syndrome and mouse models of the disorder. Further, we show that collagen type VI expression, a putative ligand of Fras1, was reduced in the PDGFRα-deficient embryonic dermis and Frem1 localization was disrupted. These results demonstrate an unexpected, essential role for PDGFRα-mediated events during dermis development and provide evidence that the dermis is required for the attachment by a mechanism that precedes disruption of Frem1 and Frem2 localization.

Materials and Methods

Mice

The mice used in this study, including the *Pdgfrα null, Pdgfrα*^{fl}, and *Pdgfrα*^{GFP} alleles *Twist2*^{Cre}, *Meox2*^{Cre} and ROSA26R mice have been described elsewhere (50, (15, 20, 24).

Histology

Antigen retrieval was utilized on paraffin sections for analysis of collagen type VI using a protease and heat denaturation protocol (48). Briefly, slides were pretreated with 0.005% acetone in 0.01N HCL at 37° C for 15 min, followed by immersion in 0.01M citrate buffer (pH 6.0) at 80° C for 2 h. Immunofluorescent analysis was performed exactly as described previously, and TEM was performed using standard methods (49). The phospho-histone H3 and TUNEL staining procedures have been described previously (20).

Antibodies

Primary antibodies and dilutions were as follows: anti-collagen type I 1:500 (Research Diagnostics), anti-collagen type III 1:500 (Calbiochem), anti-collagen type IV 1:200 (Chemicon), anti-collagen type V 1:500 (Research Diagnostics), anti-collagen type VI 1:1000 (a gift from W. Stallcup), anti-collagen type VII 1:100 (Sigma), anti-fibronectin 1:1000 (Sigma), anti-QBRICK/Frem1 3 μg/ml,

anti-Frem2 3μg/ml, anti-laminin 1:1000 (Sigma, L9393), anti-Grip1 1:100 (a gift from T. Ylikomi), anti-NG2 1:200 (a gift from W. Stallcup), anti-PDFGRα 1:1000 (Santa Cruz Biotechnology) and anti-phospho-histone H3 1:200 (Upstate). Texas red-conjugated anti-mouse, anti-rat and anti-rabbit secondary antibodies were used at a dilution of 1:100 (Molecular Probes). Alexafluor 488 and 594 anti-rabbit secondary antibodies were used at a dilution of 1:500 (Molecular Probes). Western blotting for PDGFRα was done as previously described (17).

Real-time RT-PCR

Embryonic forelimbs were dissected individually at E12.5, and total RNA was DNAse treated and purified using the RNeasy Kit with DNAse set and resuspended in 30μl of H_2O (Qiagen). Reverse transcription with 5μl of this RNA was performed with random hexamer primers with and without the addition of Superscript RT, in a total volume of 20μl, at 42° C for 2 h. Subsequently, an additional 30μl of H_2O was added to the RT reaction (Roche). Real time PCR was performed on an ABI PRISM 7000 with 2X SYBR Green master mix (Applied Biosystems), at an annealing temperature of 60° C. Each sample contained 0.25μl of cDNA in a total volume of 25μl. Primer sequences for RT-PCR are available upon request. Samples lacking RT treatment were included to control for possible genomic DNA contamination, and reaction products were analyzed by agarose electrophoresis to confirm amplification specificity. All samples were analyzed in

quadruplicate, and each primer pair was used in three separate experiments with RNA derived from at least two different litters of embryos. All replicates had crossing threshold (CT) values within 0.5 cycles. The relative expression value was derived by normalizing the quantity of the gene of interest to the quantity of GAPDH.

RT-PCR

Dorsal dermis was dissected at E16.5 and total RNA was isolated using Trizol (Invitrogen). Reverse transcription was performed with random hexamer primers and PowerScript (Clontech). Primer sequences and annealing temperatures for RT-PCR are available upon request. PCRs were run for 26 cycles.

Acknowledgements

We would like to thank B. Stallcup and T. Ylikomi for providing antibodies, and our laboratory colleagues for review of the manuscript. This research was supported in part by grants from NIH/SDRCC (AR41940-12), NIH/NHLBI (HL74257), and the March of Dimes (FY05-116) to M.D.T.

Figures

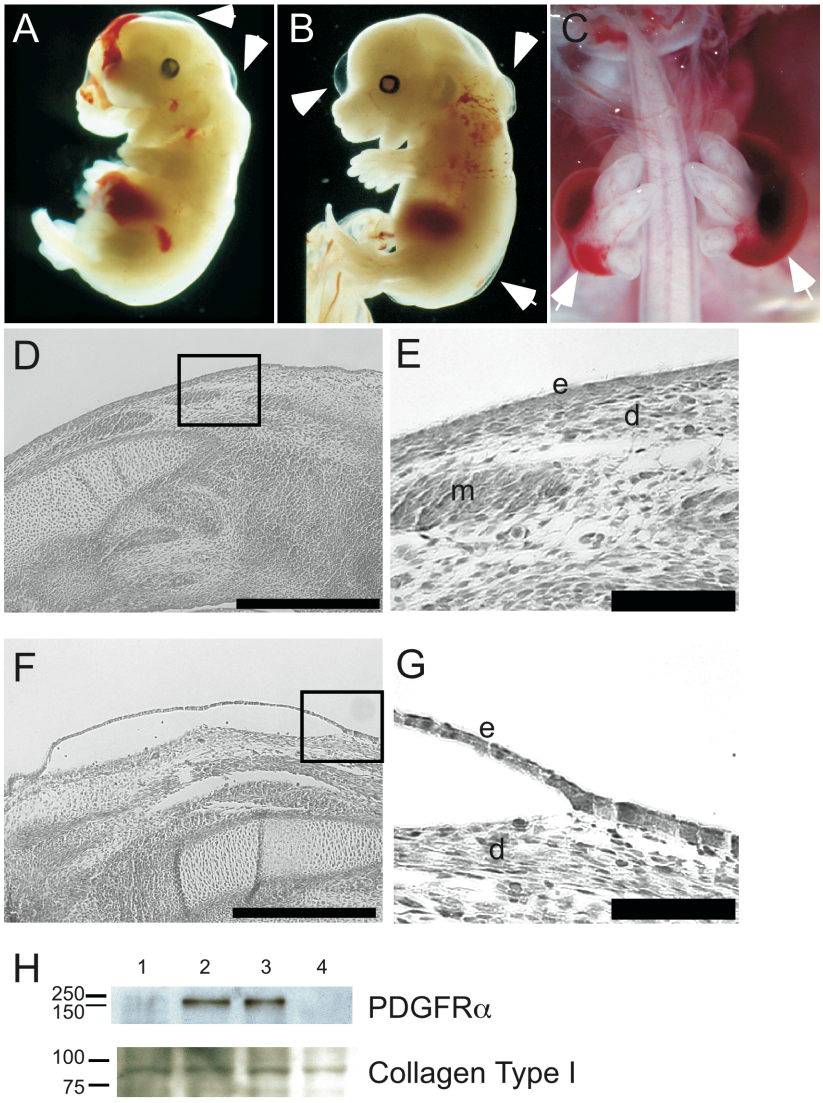

Figure 3-1. Blistering in PDGFRα deficient skin

(A-B) E13.5 and (C) E18.5 embryos deficient in PDGFRα exhibit blistering along the dorsal midline, the cranial midline, and on the dorsal aspect of the limbs. (A) Pdgfrα$^{-/-}$. (B-C) Meox2^{Cre} conditional embryos with symmetrical, blood filled, hind limb blisters. Blistering is indicated by arrows. (D-G) Limbs of E14.5 control (D-E) and PDGFRα null embryos (F-G) stained by hemotoxylin and eosin. (D, F) Paraffin sections of limb dermis and epidermis. Scale bar = 0.5 mm (E, G) Close-up image of area indicated in the box area in D and F. Scale bar = 0.1 mm. e, epidermis; d, dermis; and m, muscle. (H) Western blot analysis of PDGFRα protein levels from E15.5 limbs. Lanes 1, 4 were from Meox2^{Cre}; conditional embryos and lanes 2-3 were from PDGFRα$^{fl/GFP}$ embryos. Type I collagen was used as a loading control.

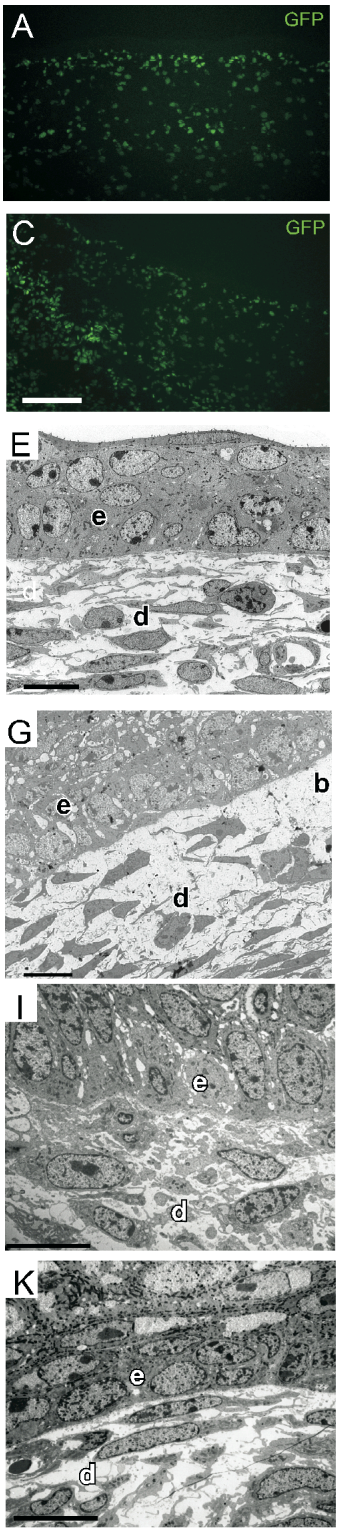

Figure 3-2. Dermal fibroblasts and basement membrane in PDGFRα mutant limb skin

(A-D) Frozen sections of E14.5 limb skin from embryos containing one $Pdgfr\alpha^{GFP}$ allele. PDGFRα expression (green) can be followed using nuclear-localized GFP inserted at the *Pdgfrα* locus (24). (A and B) $Pdgfr\alpha^{GFP/+}$ (C and D) $Meox2^{Cre/+}$; $Pdgfr\alpha^{GFP/fl}$. Laminin (red) was used to designate the basement membrane between the epidermis and the dermis. Abundant fibroblasts were observed in the dermis in both genotypes. These limb sections are representative of at least three independent embryos of each genotype. Scale bar = 0.1 mm. (E-H) TEM of E15.5 skin of (E and F) wild type and (G and H) $Meox2^{Cre/+}$ $Pdgfr\alpha^{GFP/fl}$. (E and G) Scale bar, 10 μm. (F and H) Higher magnification of E15.5 skin from E and G, respectively. H is in the region of the blister demonstrating an intact basal lamina. Scale bar = 100 nm. Arrowheads indicate lamina densa. (I-L) TEM of E18.5 dorsal skin (I and J) littermate control and (K and L) $Twist2^{Cre/+}$; $Pdgfr\alpha^{fl/fl}$. (I, K) Scale bar, 10 μm. (J, L) Scale bar, 1.0 μm.; e, epidermis; d, dermis; hd, hemidesmosomes; and col, fibrillar collagen.

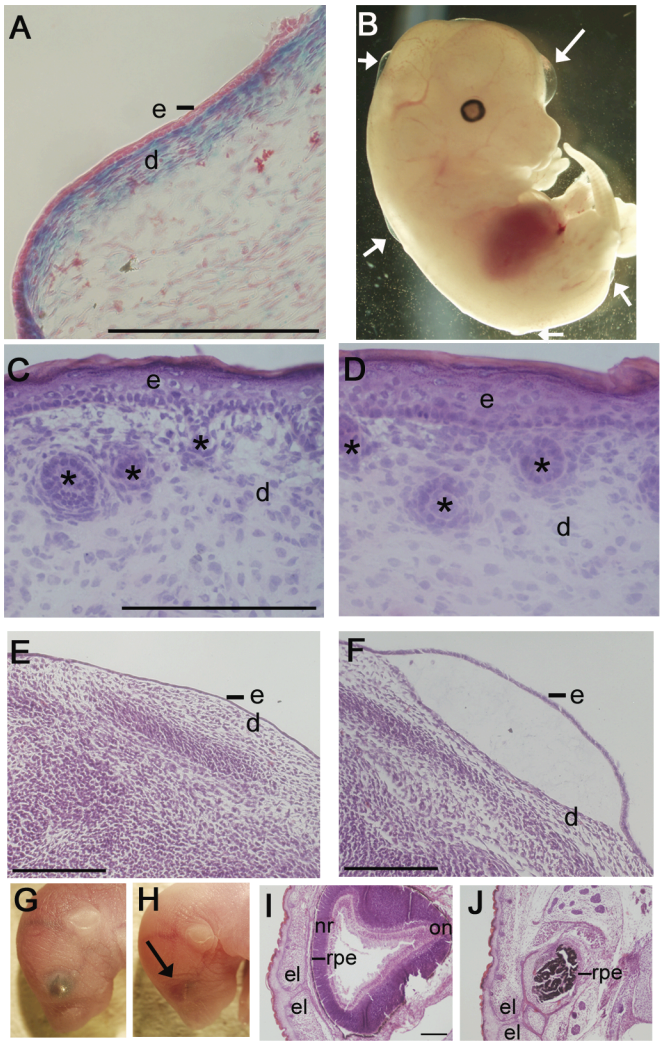

Figure 3-3. Dermal deletion of the PDGFRα results in a Fraser syndrome-like phenotype
(A) E14.5 limb section of *Twist2*^{Cre} embryo using R26R LacZ expression to indicate tissue with Cre activity. (B) E14.5 PDGFRα; *Twist2*^{Cre} conditional. Arrows point to blisters. H&E stained dorsal dermis from (C) control and (D) *Twist2*^{Cre}; PDGFRα conditional at E18.5. Asterisks indicate hair follicles. (E and F) Sections through E13.5 limbs of littermate and *Twist2*^{Cre}; PDGFRα conditional embryos. (G and H) Whole mount and (I and J) sections of (G and I) wild type and (H and J) *Twist2*^{Cre}; PDGFRα conditional eyes. e, epidermis; d, dermis; el, eyelid; rpe, retinal pigmental epithelium; nr, neural retina; and on, optic nerve. Scale bars = 100 μm.

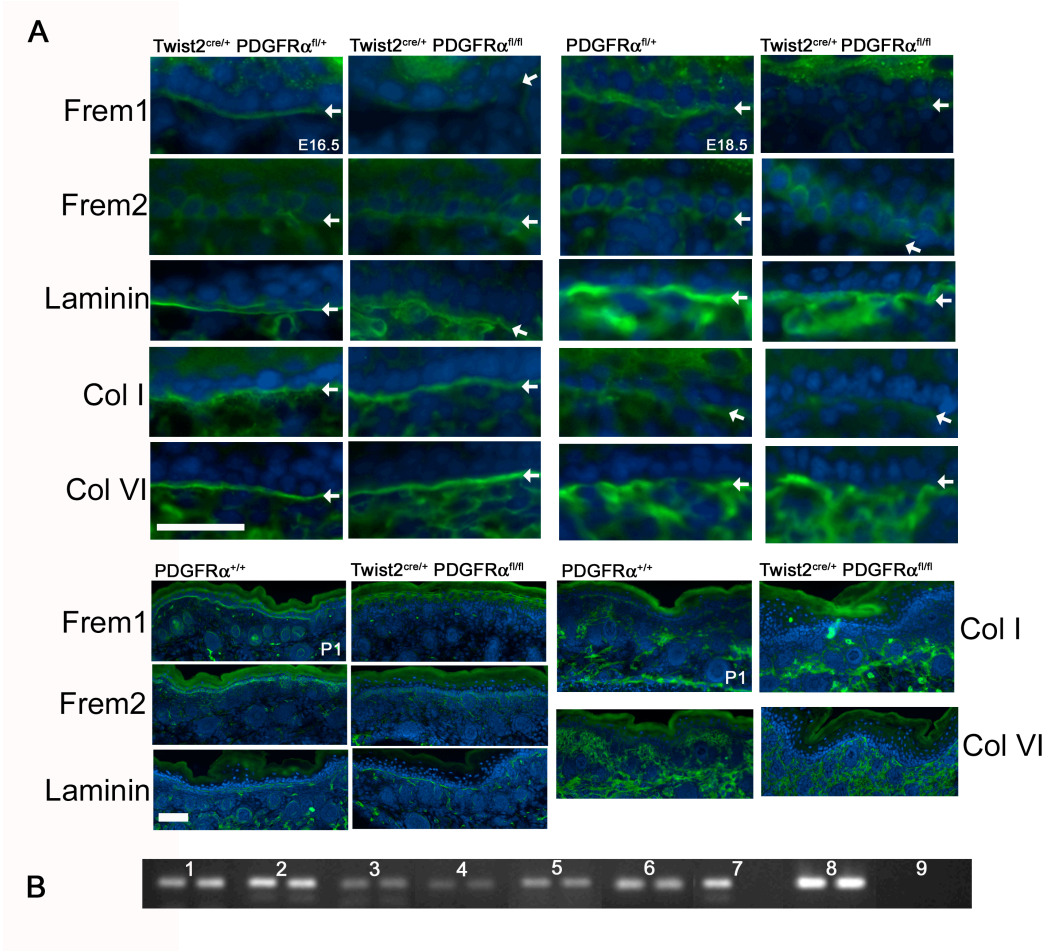

Figure 3-4. Frem1 protein was mislocalized in the absence of PDGFRα

(A) Dorsal dermis at the indicated age stained for dermal/epidermal border proteins. Sections were stained by antibodies that recognized the proteins as indicated on the left. Control embryos in left column and dermal conditional embryos in right column. Arrows indicate basement membrane between epidermis and dermis. For E16.5 and E18.5 scale bar = 20 μm and for P1 scale bar = 50 μm **(B)** Semiquantitative RT PCR from E16.5 dorsal skin. Left column of each set was from littermate and right column was from *Twist2*^{Cre};PDGFRα$^{fl/fl}$. 1, Fras1; 2, Frem1; 3, Frem2; 4, Grip1; 5, Col1a1; 6, Col4a1; 7, PDGFRα; 8, HPRT; and 9, no RT control.

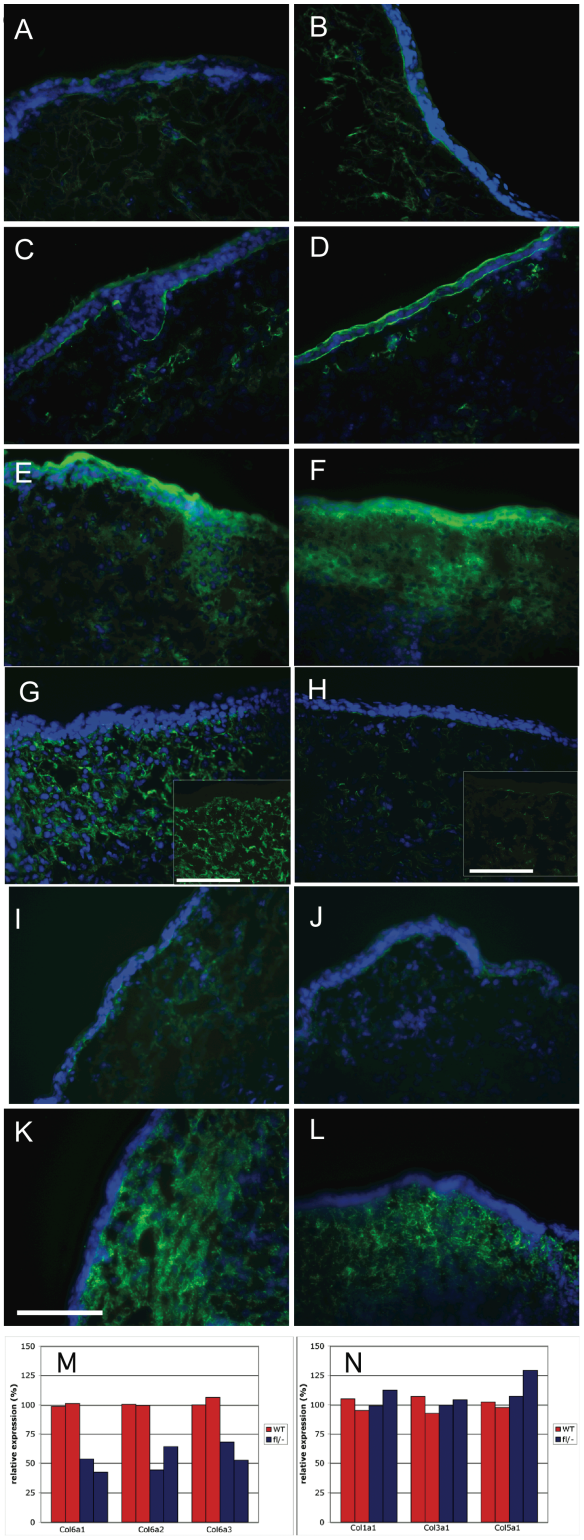

Figure 3-5. Extracellular matrix in PDGFRα deficient dermis

Immunofluorescent analysis of (A, C, E, G, I, K) P*dgfrα*$^{+/GFP}$ and (B, D, F, H, J, L) *Meox2*^{Cre}*; Pdgfrα*$^{fl/GFP}$ limb skin at E15.5. Blue, DAPI; green, Cy5 channel pseudo-colored green for detection of the matrix molecules as indicated. Insets in G and H are collagen VI staining in absence of DAPI to visualize the basement membrane localization of type VI collagen. Scale bar = 0.1 mm. Immunofluorescent image exposure times for each matrix protein were the same for mutant and control sections. (M) Expression of *COL6A1, COL6A2* and *COL6A3* mRNAs were reduced in E12.5 *Meox2*^{Cre}*; Pdgfrα*$^{fl/GFP}$ embryonic forelimbs. (N) Expression of *COL1A1, COL3A1* or *COL5A1* mRNAs was not affected. Blue bars, *Pdgfrα*$^{fl/+}$. Red bars, *Meox2*^{Cre}*;Pdgfrα*$^{fl/GFP}$. Gene expression was determined by real time RT-PCR and normalized by simultaneous amplification of *GAPDH*. Data shown represents results from two independent embryos of each genotype in two separate litters.

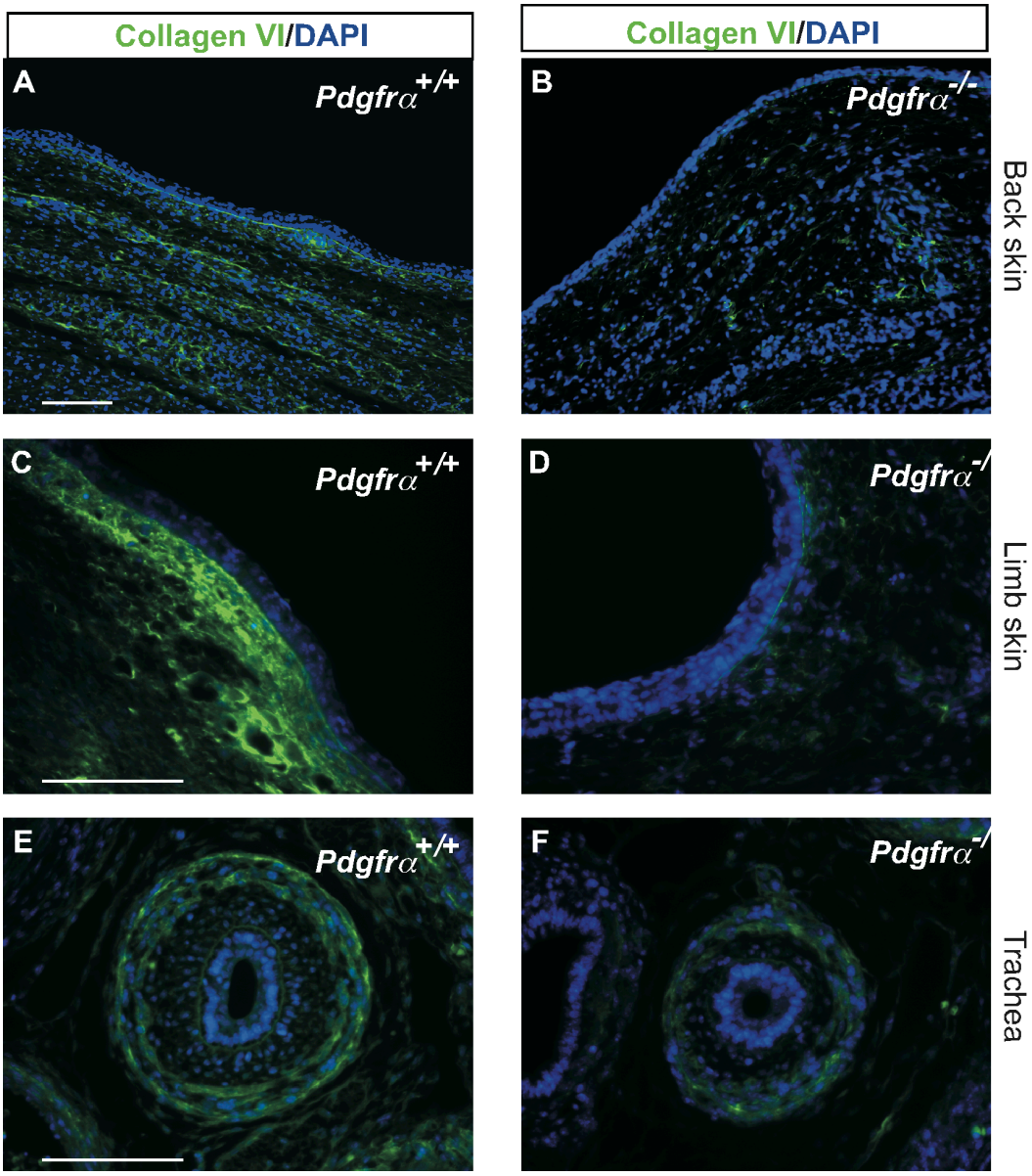

Figure 3-6. Collagen type VI expression in PDGFRα null embryos

Collagen type VI expression (pseudo-colored green) in paraffin sections of E11.5 tissues from (A, C, E) wild type and (B, D, F) *Pdgfrα*$^{-/-}$ mutant embryos. Collagen type VI was reduced on the skin of the back (A, B) and limbs (C, D) but not the trachea (E, F) of *Pdgfrα*$^{-/-}$ embryos. Arrows indicate the dermis layer in the limb. Scale bar= 0.1mm.

Table 3-1. ^{3}H Thymidine Incorporation of Primary Dermal Fibroblasts

Trial	Serum (%)		PDGF-AA (ng/ml)			bFGF (ng/ml)			TGFβ (ng/ml)
	0.1	10	0.5	5	50	0.5	5	50	5
1	134 +/- 41	1726 +/- 252	199 +/- 25	164 +/- 48	233 +/- 44	n.d.	1611 +/- 301	1231 +/- 341	123 +/- 17
2	313 +/- 47	5040 +/- 800	573 +/- 141	1231 +/- 223	724 +/- 91	1148 +/- 487	2617 +/- 691	2878 +/- 519	n.d.

Primary Dermal Fibroblast Proliferation

Cells were generated from the skin of postnatal day 1 (P1) wild type and P*dgfr*$\alpha^{GFP/+}$ mice. Skin was isolated from the thoracic region of the mice and plated dermal side down on culture dishes in DMEM, 10% FBS, antimycotic, and antibiotic. Dermal fibroblasts were allowed to migrate from the tissue for 3-4 days. Epidermis was then removed and dermal fibroblasts grown until confluent. Cells were used in assays between passage 3 and passage 10. For proliferation analysis cells were plated at $3x10^{4}$ cells per well in DMEM + 10% FBS and incubated at 37°C for 24 h. Wells were rinsed 3 times with PBS. Cells were starved in DMEM + 0.1% FBS for 24 h, and then stimulated with ligand diluted in starvation media for 18 h. Medium was replaced with DMEM + 5% FBS + 1.25 μCi/mL ^{3}H-thymidine and cells were incubated for 6 h. Wells were rinsed 2X with PBS, 2X with 5% trichloroacetic acid on ice, and lysed in 0.25 N NaOH. Incorporation of ^{3}H-thymidine was measured by scintillation counting. Samples were done in triplicate.

References

1. McGregor, L., Makela, V., Darling, S. M., Vrontou, S., Chalepakis, G., Roberts, C., Smart, N., Rutland, P., Prescott, N., Hopkins, J., Bentley, E., Shaw, A., Roberts, E., Mueller, R., Jadeja, S., Philip, N., Nelson, J., Francannet, C., Perez-Aytes, A., Megarbane, A., Kerr, B., Wainwright, B., Woolf, A. S., Winter, R. M. & Scambler, P. J. (2003) *Nat Genet* **34,** 203-8.
2. Gattuso, J., Patton, M. A. & Baraitser, M. (1987) *J Med Genet* **24,** 549-55.
3. Vrontou, S., Petrou, P., Meyer, B. I., Galanopoulos, V. K., Imai, K., Yanagi, M., Chowdhury, K., Scambler, P. J. & Chalepakis, G. (2003) *Nat Genet* **34,** 209-14.
4. Winter, R. M. (1990) *Clin Genet* **37,** 494-5.
5. Center, E. M. (1977) *Genetics Research* **29,** 147-157.
6. Bladt, F., Tafuri, A., Gelkop, S., Langille, L. & Pawson, T. (2002) *Proc Natl Acad Sci U S A* **99,** 6816-21.
7. Smyth, I., Du, X., Taylor, M. S., Justice, M. J., Beutler, B. & Jackson, I. J. (2004) *Proc Natl Acad Sci U S A* **101,** 13560-5.
8. Takamiya, K., Kostourou, V., Adams, S., Jadeja, S., Chalepakis, G., Scambler, P. J., Huganir, R. L. & Adams, R. H. (2004) *Nat Genet* **36,** 172-7.
9. Jadeja, S., Smyth, I., Pitera, J. E., Taylor, M. S., van Haelst, M., Bentley, E., McGregor, L., Hopkins, J., Chalepakis, G., Philip, N., Perez Aytes, A., Watt, F. M., Darling, S. M., Jackson, I., Woolf, A. S. & Scambler, P. J. (2005) *Nat Genet* **37,** 520-5.
10. Hoch, R. V. & Soriano, P. (2003) *Development* **130,** 4769-84.
11. Takakura, N., Yoshida, H., Kunisada, T., Nishikawa, S. & Nishikawa, S. I. (1996) *J Invest Dermatol* **107,** 770-7.
12. Karlsson, L., Bondjers, C. & Betsholtz, C. (1999) *Development* **126,** 2611-21.
13. Ding, H., Wu, X., Kim, I., Tam, P. P., Koh, G. Y. & Nagy, A. (2000) *Mech Dev* **96,** 209-13.
14. Ansel, J. C., Tiesman, J. P., Olerud, J. E., Krueger, J. G., Krane, J. F., Tara, D. C., Shipley, G. D., Gilbertson, D., Usui, M. L. & Hart, C. E. (1993) *J Clin Invest* **92,** 671-8.
15. Soriano, P. (1997) *Development* **124,** 2691-700.
16. Ding, H., Wu, X., Bostrom, H., Kim, I., Wong, N., Tsoi, B., O'Rourke, M., Koh, G. Y., Soriano, P., Betsholtz, C., Hart, T. C., Marazita, M. L., Field, L. L., Tam, P. P. & Nagy, A. (2004) *Nat Genet* **36,** 1111-6.
17. Klinghoffer, R. A., Hamilton, T. G., Hoch, R. & Soriano, P. (2002) *Dev Cell* **2,** 103-13.

18. Morrison-Graham, K., Schatteman, G. C., Bork, T., Bowen-Pope, D. F. & Weston, J. A. (1992) *Development* **115,** 133-42.
19. Payne, J., Shibasaki, F. & Mercola, M. (1997) *Dev Dyn* **209,** 105-16.
20. Tallquist, M. D. & Soriano, P. (2003) *Development* **130,** 507-18.
21. Gruneberg, H. & Truslove, G. (1960) *Genetics Research* **1,** 69-90.
22. Orr-Urtreger, A. & Lonai, P. (1992) *Development* **115,** 1045-58.
23. Schatteman, G. C., Morrison-Graham, K., van Koppen, A., Weston, J. A. & Bowen-Pope, D. F. (1992) *Development* **115,** 123-31.
24. Hamilton, T. G., Klinghoffer, R. A., Corrin, P. D. & Soriano, P. (2003) *Mol Cell Biol* **23,** 4013-25.
25. Tallquist, M. D. & Soriano, P. (2000) *Genesis* **26,** 113-5.
26. Allen, E., Piontek, K. B., Garrett-Mayer, E., Garcia-Gonzalez, M., Gorelick, K. L. & Germino, G. G. (2006) *Hum Mol Genet* **15,** 11-21.
27. Morris, S. M., Tallquist, M. D., Rock, C. O. & Cooper, J. A. (2002) *Embo J* **21,** 1555-64.
28. Lu, C. C. & Robertson, E. J. (2004) *Dev Biol* **273,** 149-59.
29. Ishikawa, O., LeRoy, E. C. & Trojanowska, M. (1990) *J Cell Physiol* **145,** 181-6.
30. Lubinus, M., Meier, K. E., Smith, E. A., Gause, K. C., LeRoy, E. C. & Trojanowska, M. (1994) *J Biol Chem* **269,** 9822-5.
31. Kazlauskas, A., Bowen-Pope, D., Seifert, R., Hart, C. E. & Cooper, J. A. (1988) *Embo J* **7,** 3727-35.
32. Amano, S., Ogura, Y., Akutsu, N. & Nishiyama, T. (2007) *Exp Dermatol* **16,** 151-5.
33. Gabele, E., Reif, S., Tsukada, S., Bataller, R., Yata, Y., Morris, T., Schrum, L. W., Brenner, D. A. & Rippe, R. A. (2005) *J Biol Chem* **280,** 13374-82.
34. Smith, L. T. (1994) *Matrix Biol* **14,** 159-70.
35. Keene, D. R., Engvall, E. & Glanville, R. W. (1988) *J Cell Biol* **107,** 1995-2006.
36. Bonaldo, P., Braghetta, P., Zanetti, M., Piccolo, S., Volpin, D. & Bressan, G. M. (1998) *Hum Mol Genet* **7,** 2135-40.
37. Li, L., Cserjesi, P. & Olson, E. N. (1995) *Dev Biol* **172,** 280-92.
38. Timmer, J. R., Mak, T. W., Manova, K., Anderson, K. V. & Niswander, L. (2005) *Proc Natl Acad Sci U S A* **102,** 11746-50.
39. Nguyen, M. & Arnheiter, H. (2000) *Development* **127,** 3581-91.
40. Smyth, I. & Scambler, P. (2005) *Hum Mol Genet* **14 Spec No. 2,** R269-74.
41. Kiyozumi, D., Sugimoto, N. & Sekiguchi, K. (2006) *Proc Natl Acad Sci U S A* **103,** 11981-6.
42. Tallquist, M. D., Weismann, K. E., Hellstrom, M. & Soriano, P. (2000) *Development* **127,** 5059-70.

43. Aase, K., Abramsson, A., Karlsson, L., Betsholtz, C. & Eriksson, U. (2002) *Mech Dev* **110,** 187-91.
44. Fredriksson, L., Li, H., Fieber, C., Li, X. & Eriksson, U. (2004) *Embo J* **23,** 3793-802.
45. Li, X., Ponten, A., Aase, K., Karlsson, L., Abramsson, A., Uutela, M., Backstrom, G., Hellstrom, M., Bostrom, H., Li, H., Soriano, P., Betsholtz, C., Heldin, C. H., Alitalo, K., Ostman, A. & Eriksson, U. (2000) *Nat Cell Biol* **2,** 302-9.
46. Rodt, S. A., Ahlen, K., Berg, A., Rubin, K. & Reed, R. K. (1996) *J Physiol* **495 (Pt 1),** 193-200.
47. Bonner, J. C. (2004) *Cytokine Growth Factor Rev* **15,** 255-73.
48. Ezaki, T. (2000) *Micron* **31,** 639-49.
49. Anderson, R., Fassler, R., Georges-Labouesse, E., Hynes, R. O., Bader, B. L., Kreidberg, J. A., Schaible, K., Heasman, J. & Wylie, C. (1999) *Development* **126,** 1655-64.

CHAPTER FOUR

A Role for PDGF Receptor Signaling in Bone Development

Introduction

The Platelet Derived Growth Factor (PDGF) signaling network has been previously shown to have a role in skeletal development. Platelet derived growth factor receptor (PDGFR) α null embryos possess numerous skeletal defects including failed fusion of the nasal bones at the midline, underdeveloped acromion of the scapula, rib fusions and bifurcations, irregular sternal bands, and spina bifida (1). Many of these defects are recapitulated in $PDGFA^{-/-};PDGFC^{-/-}$ mutant mice (2). Much of the previous research on these defects has focused on an early role for PDGF signaling.

PDGF-A and PDGFRα have been implicated in the patterning of the somites. During development the myotome expresses both PDGFAA and PDGFCC ligands while the sclerotome expresses PDGFRα (3-6). Because the sclerotome gives rise to the bones of the axial skeleton, defects in rib formation have been attributed as a consequence of faulty somite patterning. However, PDGF signaling is not restricted to a role solely in this early developmental stage. Chondrocytes, osteoblasts, and perichondrial cells have all been shown to express PDGFR or to respond to PDGF stimulation in culture (7-9). In these studies, PDGF treatment has induced chondrogenesis in micromass cultures and stimulated proliferation in chondrocytes and osteoblasts (10, 11).

One of the major molecular effectors downstream of PDGFR is phosphoinositide 3-kinase (PI3K). PI3K signaling has demonstrated roles in

osteoblast proliferation, survival, and differentiation and a suggested role in osteoclast migration (12-15). In vitro analysis has implicated PI3K signaling downstream of a number of growth and differentiation factors including FGF2, HPG, IGF, BMP2, as being involved in chondrocyte differentiation, proteoglycan synthesis, and survival (16-19). This project seeks to determine the role of PDGF and PI3K signaling in bone development utilizing mutant mice deficient in PI3K signaling downstream of the PDGFRs and tissue-specific conditional mutant mice with PDGFR deletion in the chondrocytes.

Results

PI3K signaling downstream of both receptors is required for embryonic survival

To investigate the requirement for PI3K signaling downstream of both receptors, and to determine in which tissues PDGFRβ is functionally redundant and capable of partially rescuing deficient PDGFRα signaling, we crossed signaling point mutant mice deficient in PI3K signaling downstream of PDGFRα and PDGFRβ. Isolations from timed matings produced offspring in Mendelian ratios up to e14.5. Isolations at later time points yielded only one double mutant embryo (at e17.5), and no pups with a double mutant genotype were ever born, indicating embryonic lethality. Double mutant embryos displayed facial clefting, along with hemorrhagic blebbing in the craniofacial and trunk region (as previously reported in (20) and Fig 1). Approximately 40% of embryos isolated had severe pericardial effusion (Fig 1c). Since PDGFR$\alpha^{PI3K/PI3K}$ embryos survive until birth and PDGFR$\beta^{PI3K/PI3K}$ are viable, these data indicate that PI3K signaling downstream of PDGFRβ is capable of partially rescuing deficiencies downstream of PDGFRα.

Lack of PI3K signaling leads to disorganized chondrocyte populations and somite survival defect

We decided to focus on bone development in these mutants because little is known about the role of PDGF and PI3K signaling in these tissues in vivo. Analysis of H&E stained serial sections revealed a disorganization of the chondrocytes of the vertebral body, ribs, and scapula, but not in the chondrocyte populations of developing long bone (Fig 2). These disorganized populations had a lower density of cells and a reduction in cell-cell contact. Cell morphology and Col2a in situ hybridization results indicated that the disorganized populations were, in fact, differentiated chondrocytes and not undifferentiated sclerotome (Fig 2C-D).

Since the vertebral bodies, ribs, and scapula are somite-derived tissues, we looked at an earlier stage to determine if there were defects in the somites. Because PI3K is known to play a role in cell survival, we performed whole mount TUNEL on e10.5 embryos. Interestingly, the double mutant embryos showed a marked increase in apoptosis within the somites (Fig 3). This increase in cell death does not appear to be spread throughout the entire somite, but instead is localized to a specific region, potentially the sclerotome.

PDGFRα and PDGFRβ expression patterns partially overlap in developing bone

We analyzed the expression patterns of α and β in the developing bone to determine where and when the two receptors might have overlapping or compensatory function. Using PDGFRα^{GFP} (which expresses GFP from the PDGFRα locus) and a PDGFRβ antibody, we determined that PDGFRα was strongly expressed in the sclerotome portion of the somite (as previously reported in (1)), as well as in the proliferative chondrocytes. PDGFRα expression was then reduced as chondrocytes further differentiate, but was maintained strongly in the perichondrium. PDGFRβ expression appeared to increase within the developing bone as the chondrocytes matured. (Fig 4). This changing pattern of PDGFRα and PDGFRβ within the developing vertebral column suggests that each receptor plays a differential, time-dependent role.

Chondrocyte-specific deletion of PDGFRα

The embryonic lethality of PDGFRα$^{PI3K/PI3K}$; β$^{PI3K/PI3K}$ embryos by e14.5 precludes analysis of late stage bone development. Because both receptors were expressed in cell populations of the developing bone at later stages, we hypothesized that they also played a second, later role in embryonic development. To determine the effects of the loss of both receptors on bone development, we

utilized the cre-lox system driven by Col2a1 to specifically delete the receptors in chondrocytes (indicated by CKO).

PDGFRα^{CKO} embryos survived to birth but died shortly thereafter from a cleft palate. Skeletal preparations of these embryos and pups revealed that the PDGFRα^{CKO} mutants presented two additional phenotypes: a misaligned sternum (Fig 5) and bones that were more brittle than those of littermate controls (as observed while performing dissections of skeletal preparations). The sternum defect (previously described in the literature as a "crankshaft sternum" (21)) was present in equal severity in 66% of PDGFRα^{CKO} embryos and pups.

Late-stage bone defects

Skeletal preparations from PDGFRα^{CKO}; β^{CKO} embryos displayed a cleft palate and sternum alignment defect identical to that seen in the PDGFRα^{CKO} mutants. Comparison of long bones with littermate controls revealed no gross abnormalities. Serial sectioning of a PDGFRα^{CKO}; β^{CKO} embryo showed chondrocyte disorganization of the vertebral body at e15.5 (Fig 6), similar to that observed in the PDGFRα$^{PI3K/PI3K}$; β$^{PI3K/PI3K}$ at e12.5. At this later stage, the vertebral body of the double mutant had fewer hypertrophic chondrocytes than that of the littermate control. Additionally, initial observation of sections through long bone revealed a potential expansion of the growth plate at this time point in double mutant embryos compared to littermate controls (Fig 6C-D).

Discussion

These findings show that PI3K signaling downstream of PDGFRα and PDGFRβ is essential for embryonic development and that there is a specific requirement for this signaling in the developing bones of the axial skeleton. Previous studies reported rib fusions and variably penetrant scapula defects in the PDGFR$\alpha^{PI3K/PI3K}$; $\beta^{PI3K/PI3K}$ mutant embryos (20). While no gross differences of this kind were observed in our mutants, we did see a disorganization of the chondrocytes within the developing ribs and scapula.

Increased apoptosis within the somites of PDGFRα null embryos at e10.5 was previously reported (1), though serial sectioning revealed that while there was some cell death occurring within the sclerotome, the majority was found in the dermomyotome. Our findings indicate that PI3K signaling downstream of the receptors plays a significant role in cell survival. Determination of which somite subcompartment is most affected in our mutants will give further clues as to whether later stage bone defects could be the result of a primary survival defect in this precursor population.

The disorganization of the chondrocytes within the vertebral body suggests a potential change in the developmental programming of that cell population. Normally, the cells of the vertebral body maintain a tight, organized, condensed pattern around the regressing notochord, while the cells of the developing intervertebral disc appear more loosely joined as they surround the

notochord as it becomes the nucleus pulposus. This differential cell patterning begins when two somite halves fuse to form the single vertebral column component. The cells of the upper half, which will form the future vertebral body, are considerably more dense that the cells in the lower half, which will go on to form the intervertebral disc. Given the potential increase in apoptosis within the developing somite of mutant embryos, it is possible that the upper half of the somite is starting out with fewer cells and thus a sparse, disorganized patterning similar that that of the lower half. Alternatively, this phenotype could be the result of altered PDGF signaling leading to an early differentiation of the chondrocytes within the vertebral body as we observe an increase in the number of hypertrophic chondrocytes present at e15.5. Analyzing markers of differentiation at earlier time points by in situ hybridization will determine when this early differentiation begins.

While there is definitely an early role of survival there could also be this late role for the PDGFRs in differentiation. Signaling is needed for survival of some sclerotome cells. Failure of these cells to survive could lead to fewer chondrocytes. Since endochondral ossification has feedback regulation, loss of some cells early could lead to differentiation defects later as a secondary effect. And what about the perichondrium? Given the consistent, strong expression of PDGFRα in the perichondrium, there must be a role for it in bone development. The function of the perichondrium is still poorly understood, though Karsenty

(22) makes a case for its involvement in regulation of chondrocyte maturation through transcriptional inhibition via Runx2 and FGF18. Given that PDGFRα is upstream of forkhead transcription factors it is possible that PDGFRα could also be exerting such control.

The misaligned sternum defect, in varying degrees of severity, has been reported in other mutants: the homeobox-containing gene, *Engrailed-1* null (23), the Polycomb group genes compound mutant, *bmi1-/-M33+/-* (24), haploinsufficiency of the forkhead transcription gene, *Foxfl+/-* (25), *BMP4+/- BMP7+/-* double heterozygote mutant (26), and a transcription factor downstream of PDGFR, *Mzf6d* null (27). While no direct mechanism has been uncovered for this phenotype, circumstantial evidence points predominately toward failure of proper BMP signaling. The sternal bands migrate from the sclerotome portion of the somite along with the ribs. Therefore, it is most likely that the phenotype is occurring due to a defect in the cells' abilities to migrate along the correct path. We observed this type of function for PDGFR signaling in a dorsal mesenchyme population (see chapter 2). Failure of those cells to migrate resulted in the development of spina bifida.

In conclusion, these data indicate an important role in bone development for PI3K downstream of the PDGFRs. Given the many cell functions in which PI3K is known to play a role, it is likely that these signaling events occur both early and late in development.

Materials and Methods

Mice

The mutant and Cre alleles used in these experiments were: *PDGFRα*^{F2} (20), PDGFRβ^{F2} (Heuchel et al. 1999), *PDGFRα*^{GFP} (28), *PDGFRα*^{fl} (29), PDGFRβ^{fl} (AMR and MDT unpublished reagent), and *Col2a1-Cre*^{Tg} (30). The *Col2a1-Cre*^{Tg} mice were kindly provided by G. Karsenty. Embryos possessing a tissue specific deletion of the PDGFRα/β were generated by crossing males (PDGFRα$^{fl/+}$; PDGFRβ$^{fl/+}$ Cre^{+}) to females homozygous for the PDGFRα$^{fl/fl}$; β$^{fl/fl}$.

Histological procedures and skeletal staining

For H&E and Safranin-O staining embryos were fixed in 4% paraformaldehyde at 4°C overnight, embedded in paraffin, sectioned at a thickness of 7 μm, and stained according to standard procedures. Skeletal preparations were performed according to (31). For RNA in situ analysis and green fluorescent protein (GFP) expression embryos were fixed in 4% PFA overnight, saturated in 10% sucrose at 4°C overnight, embedded in OCT, and sectioned at 14 μm or 10 μm, respectively. In situ analyses were performed as previously described (32). TUNEL analysis was performed by standard procedures using biotinylated-14-dATP and detected

using the strepavidin-HRP and DAB (Vectastain) kits. For PDGFRβ antibody staining…

Figures

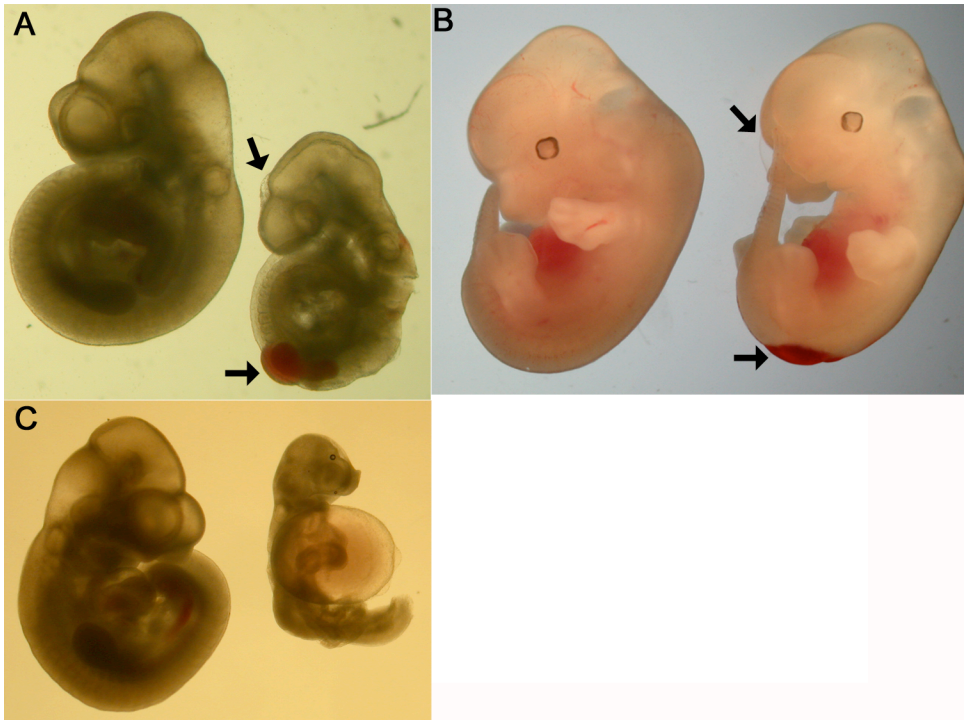

Figure 4-1. PDGFRα$^{PI3K/PI3K}$; β$^{PI3K/PI3K}$ phenotype
Mutant embryos displayed hemorrhagic blebs **(A,B)** and craniofacial clefting **(B)**. Some mutant embryos presented pericardial effusion **(C)**. Double mutant embryos (left) and littermate controls (PDGFRβ$^{PI3K/PI3K}$, on right). Arrows point to blebs. **(A,C)** E10.5, **(B)** E13.5.

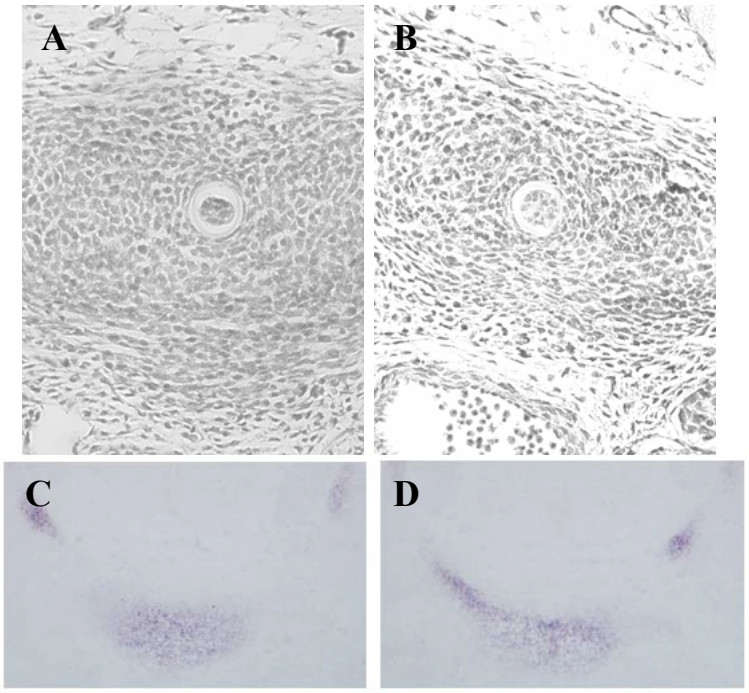

Figure 4-2. Disorganization of vertebral body chondrocytes
Chondrocytes of vertebral bodies at E12.5 were disorganized and had a lower cell density in the PDGFR$\alpha^{PI3K/PI3K}$; $\beta^{PI3K/PI3K}$ mutant **(B)** compared to littermate control **(A)**. In situ hybridization for Type II collagen, a marker for chondrocytes, indicated the vertebral body cells were at similar differentiated states **(C,D)**.

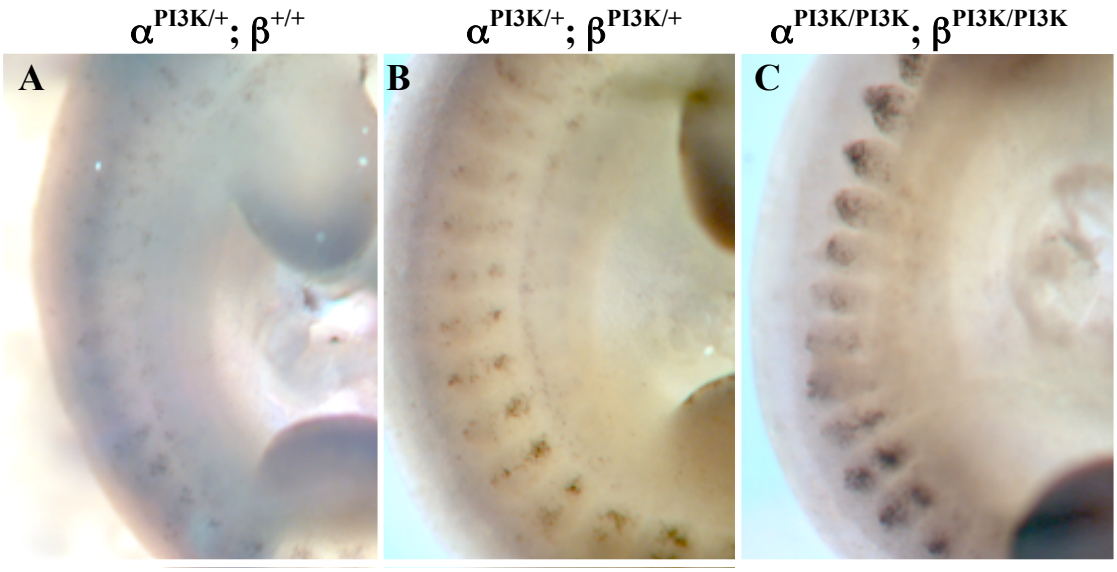

Figure 4-3. Increased apoptosis within the somites
E10.5 double mutant embryos **(C)** had increased apoptosis of the somites compared to single and double heterozygous controls **(A,B)**.

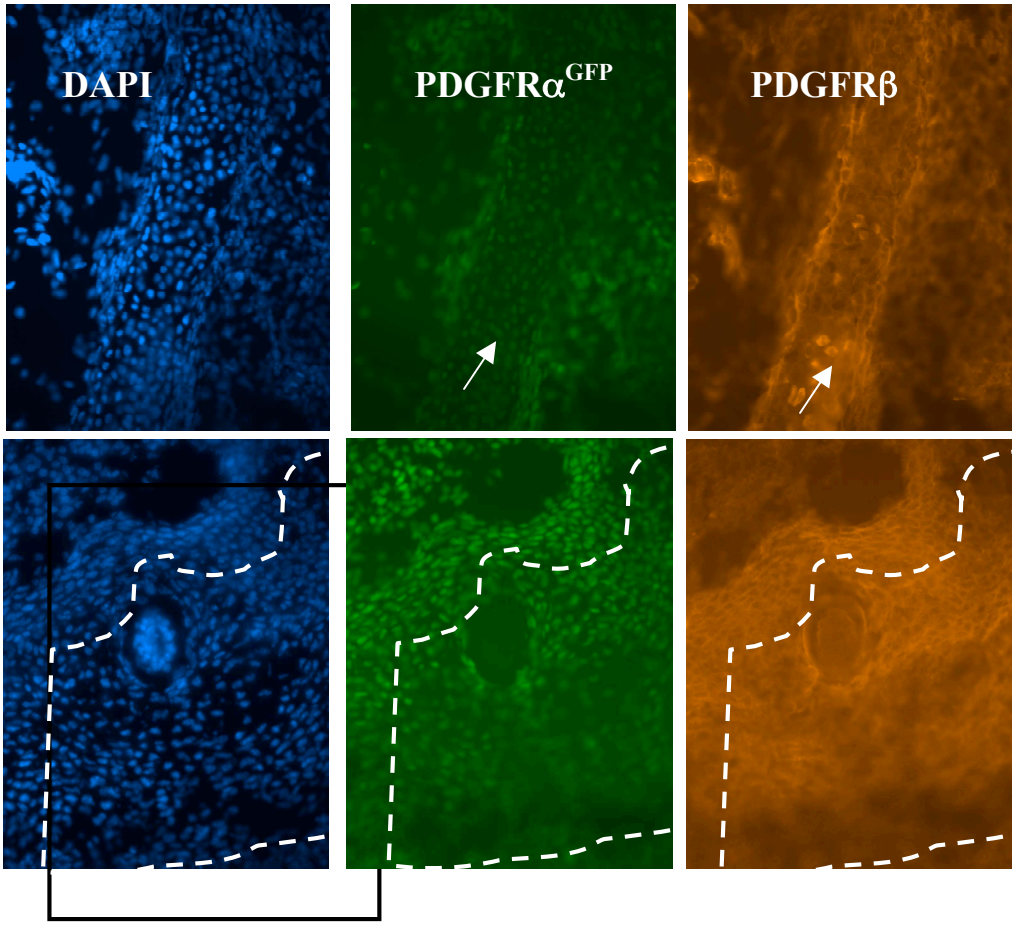

Figure 4-4. Coexpression of PDGFRα and PDGFRβ in vertebral body and arch at E14.5
PDGFRα and PDGFRβ were co-expressed in the perichondrium of the vertebral arch (top panels) and some chondrocytes of the vertebral body (bottom panels). Arrows point to perichondrium.

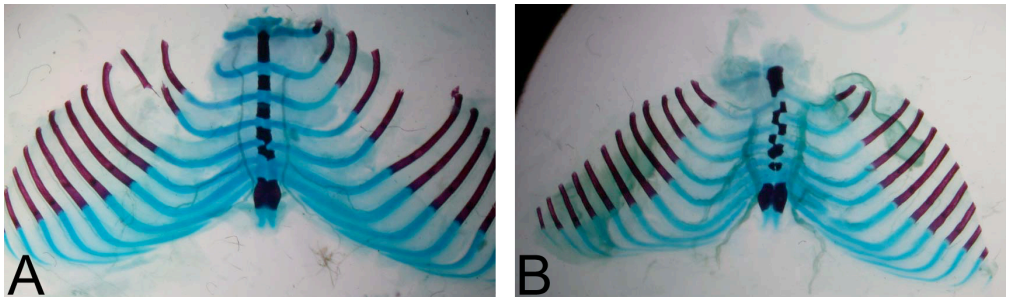

Figure 4-5. Sternum alignment defect in PDGFRα^{CKO}
The sternal bands failed to align properly, forming a checkerboard pattern, in the PDGFRα^{CKO} mutant **(B)**. Littermate control **(A)**. Skeletal preps were from newborn pups.

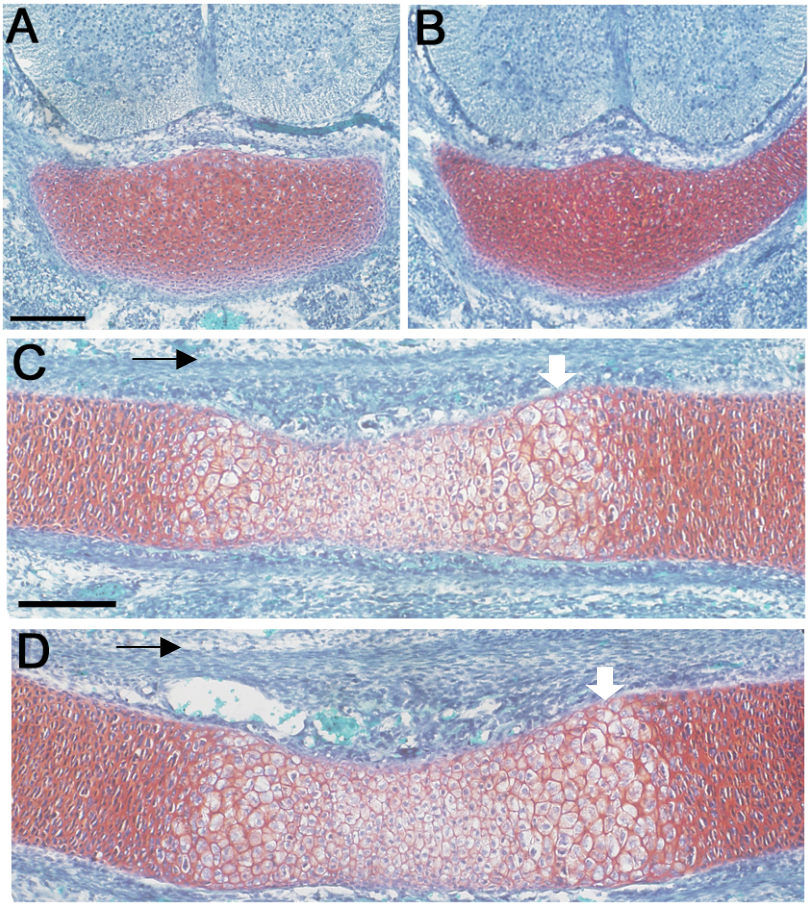

Figure 4-6. Type II Col-cre deletion of PDGFRs
E15.5 vertebral bodies **(A,B)** and long bone **(C,D)** of PDGFRα^{CKO}; β^{CKO} **(B,D)** and littermate control **(A,C)**. Safranin O staining revealed fewer hypertrophic chondrocytes in the vertebral body of the mutant, as well as disorganized perichondrium and a potential expansion of the growth plate in long bone. Safranin O stains red the cartilage matrix produced by chondrocytes. Hypertrophic chondrocytes and areas of ossification appear white. Black arrows point to perichondrium, white arrows indicated hypertrophic zone.

REFERENCES

1. Soriano, P. (1997) *Development* **124,** 2691-2700.
2. Ding, H., Wu, X., Bostrom, H., Kim, I., Wong, N., Tsoi, B., O'Rourke, M., Koh, G. Y., Soriano, P., Betsholtz, C*., et al.* (2004) *Nat Genet* **36,** 1111-1116.
3. Ding, H., Wu, X., Kim, I., Tam, P. P., Koh, G. Y., & Nagy, A. (2000) *Mech Dev* **96,** 209-213.
4. Orr-Urtreger, A., Bedford, M. T., Do, M. S., Eisenbach, L., & Lonai, P. (1992) *Development* **115,** 289-303.
5. Orr-Urtreger, A. & Lonai, P. (1992) *Development* **115,** 1045-1058.
6. Schatteman, G. C., Morrison-Graham, K., van Koppen, A., Weston, J. A., & Bowen-Pope, D. F. (1992) *Development* **115,** 123-131.
7. Arai, F., Ohneda, O., Miyamoto, T., Zhang, X. Q., & Suda, T. (2002) *J Exp Med* **195,** 1549-1563.
8. Kieswetter, K., Schwartz, Z., Alderete, M., Dean, D. D., & Boyan, B. D. (1997) *Endocrine* **6,** 257-264.
9. Zhang, L., Leeman, E., Carnes, D. C., & Graves, D. T. (1991) *Am J Physiol* **261,** C348-354.
10. Ataliotis, P. (2000) *Mech Dev* **94,** 13-24.
11. Tallquist, M. D., Weismann, K. E., Hellstrom, M., & Soriano, P. (2000) *Development* **127,** 5059-5070.
12. Almeida, M., Han, L., Bellido, T., Manolagas, S. C., & Kousteni, S. (2005) *J Biol Chem* **280,** 41342-41351.
13. Ghosh-Choudhury, N., Mandal, C. C., & Choudhury, G. G. (2007) *J Biol Chem* **282,** 4983-4993.
14. Guenou, H., Kaabeche, K., Dufour, C., Miraoui, H., & Marie, P. J. (2006) *Am J Pathol* **169,** 1303-1311.
15. Pilkington, M. F., Sims, S. M., & Dixon, S. J. (1998) *J Bone Miner Res* **13,** 688-694.
16. Debiais, F., Lefevre, G., Lemonnier, J., Le Mee, S., Lasmoles, F., Mascarelli, F., & Marie, P. J. (2004) *Exp Cell Res* **297,** 235-246.
17. Forte, G., Minieri, M., Cossa, P., Antenucci, D., Sala, M., Gnocchi, V., Fiaccavento, R., Carotenuto, F., De Vito, P., Baldini, P. M*., et al.* (2006) *Stem Cells* **24,** 23-33.
18. Lessmann, E., Grochowy, G., Weingarten, L., Giesemann, T., Aktories, K., Leitges, M., Krystal, G., & Huber, M. (2006) *Exp Hematol* **34,** 1532-1541.
19. Sugimori, K., Matsui, K., Motomura, H., Tokoro, T., Wang, J., Higa, S., Kimura, T., & Kitajima, I. (2005) *J Bone Miner Metab* **23,** 411-419.

20. Klinghoffer, R. A., Hamilton, T. G., Hoch, R., & Soriano, P. (2002) *Dev Cell* **2,** 103-113.
21. Theiler (1989) *The House Mouse: Atlas of Embryonic Development* (Springet-Verlag, New York).
22. Hinoi, E., Bialek, P., Chen, Y. T., Rached, M. T., Groner, Y., Behringer, R. R., Ornitz, D. M., & Karsenty, G. (2006) *Genes Dev* **20,** 2937-2942.
23. Wurst, W., Auerbach, A. B., & Joyner, A. L. (1994) *Development* **120,** 2065-2075.
24. Bel, S., Core, N., Djabali, M., Kieboom, K., Van der Lugt, N., Alkema, M. J., & Van Lohuizen, M. (1998) *Development* **125,** 3543-3551.
25. Mahlapuu, M., Enerback, S., & Carlsson, P. (2001) *Development* **128,** 2397-2406.
26. Katagiri, T., Boorla, S., Frendo, J. L., Hogan, B. L., & Karsenty, G. (1998) *Dev Genet* **22,** 340-348.
27. Schmahl, J., Raymond, C. S., & Soriano, P. (2007) *Nat Genet* **39,** 52-60.
28. Hamilton, T. G., Klinghoffer, R. A., Corrin, P. D., & Soriano, P. (2003) *Mol Cell Biol* **23,** 4013-4025.
29. Tallquist, M. D. & Soriano, P. (2003) *Development* **130,** 507-518.
30. Ovchinnikov, D. A., Deng, J. M., Ogunrinu, G., & Behringer, R. R. (2000) *Genesis* **26,** 145-146.
31. (1994) *Manipulating the Mouse Embryo* (Cold Spring Harbor Press, Cold Spring Harbor, NY).
32. Wilkinson, D. G. (1992) *Whole mount in situ hybridization to vertebrate embryos* (IRL Press, Oxford).

Conclusions

My results contribute data that leads to new ideas about the development of spina bifida, the role of PDGFRα in migration, and the involvement of PI3K signaling in actin filament formation and its related signaling.

A search of the scientific literature reveals more than 60 mouse models that develop spina bifida due to failure of neural tube closure. When spina bifida is discussed, it is almost always referred to as a neural tube defect. With the prevalence of folic acid supplementation in human diets in order to prevent neural tube defects, some people wrongly assume that spina bifida is no longer a problem. My results highlight a form of spina bifida that is not the result of defects in neural tube closure and is therefore likely to be insensitive to folic acid supplementation.

PDGFRα signaling is generally thought to play roles in survival and proliferation. My analysis of the function of this receptor in the dermis and the sclerotome demonstrate it plays neither of those roles in these cell types. Instead, the data points to roles in matrix production and migration, respectively. Previous microarray analysis (and in vitro studies) has established the ability of the PDGF receptors to regulate transcription of extracelluar matrix molecules such as syndecan, tenascin C, decorin, and versican. Therefore, it is not surprising that PDGFRα signaling in the dermis is required for regulation of some extracellular

matrix molecule. It is interesting that it is not required for the transcription, translation, or secretion of any of the matrix molecules known to play a role in dermal-epidermal junction maintenance, suggesting there are additional, unknown, proteins participating in this process. Migration as a result of PDGFR signaling, on the other hand, is a function largely assigned to PDGFRβ, not PDGFRα. Studies performed in vitro have focused on vascular smooth muscle cells, which do not express PDGFRα. My data demonstrates the ability of PDGFRα to induce chemotaxis in vitro as well as a role for this function in vivo.

Additionally, this data adds to the limited amount of study performed on signaling point mutations in the PDGFRα. Currently, only PDGFRα allelic series mutants exist for the PI3K and Src sites. Previously, analysis of $PDGFR\alpha^{PI3K/PI3K}$ mutant embryos determined the presence of spina bifida, but did not investigate the cause. My results define the cell population and cell function responsible for the spina bifida phenotype in these mutants.

Finally, since this is a specific signaling point mutant that blocks PI3K activity downstream of the PDGFRα, these studies provide a clearer picture of the migration function of PI3K activity downstream of a specific receptor tyrosine kinase. Previous in vitro analysis of the role of PI3K in migration has relied heavily on inhibition of PI3K by wortmannin or LY294002. This blocks all PI3K activity in the treated cells and thus may cause additional effects unrelated to the signal transduction being studied. The $PDGFR\alpha^{PI3K/PI3K}$ mutant provides not only

a specific block of PI3K signaling, but also an in vivo system in which to analyze the effect. This specificity is particularly important when it comes to the study of signaling molecules farther downstream, such as PAK1 and Rac1. Current evidence for their participation in migration via actin filament formation downstream of various growth factors comes largely from in vitro studies using drug inhibition or overexpression of dominant negative constructs.

VITAE

Elizabeth Ann (Walker) Pickett was born in San Antonio, Texas, on April 4, 1979, the daughter of Matthew and Cindy Walker. After graduating Summa Cum Laude from Theodore Roosevelt High School, San Antonio, Texas in 1997, she became a proud member of the Fightin' Texas Aggie Class of 2001 (WHOOP!) at Texas A&M University in College Station, Texas. She received the degree of Bachelor of Science with a major in genetics from Texas A&M University in May 2001. She married Mark Pickett in July of 2001 and, in August, entered the Graduate School of Biomedical Sciences at the University of Texas Southwestern Medical Center at Dallas. She was awarded the degree of Doctor of Philosophy in May of 2007.